NAVAL POSTGRADUATE SCHOOL
MONTEREY, CALIFORNIA

THESIS 19961125 092

**AN ANALYSIS OF ENERGY SPREADING LOSS
ASSOCIATED WITH TACTICAL ACTIVE SONAR
PERFORMANCE
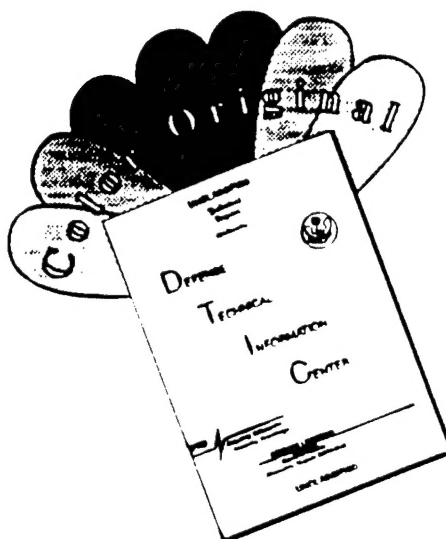IN A SHALLOW WATER ENVIRONMENT**

by

Akira Tanaka

June 1996

Thesis Advisors: Robert H. Bourke
                                    James H. Wilson

Approved for public release; distribution is unlimited

DISCLAIMER NOTICE

THIS DOCUMENT IS BEST QUALITY AVAILABLE. THE COPY FURNISHED TO DTIC CONTAINED A SIGNIFICANT NUMBER OF COLOR PAGES WHICH DO NOT REPRODUCE LEGIBLY ON BLACK AND WHITE MICROFICHE.

REPORT DOCUMENTATION PAGE

Form Approved OMB No. 0704-0188

1. AGENCY USE ONLY *(Leave blank)*	2. REPORT DATE June, 1996	3. REPORT TYPE AND DATES COVERED Master's Thesis	
4. TITLE AND SUBTITLE AN ANALYSIS OF ENERGY SPREADING LOSS ASSOCIATED WITH TACTICAL ACTIVE SONAR PERFORMANCE IN A SHALLOW WATER ENVIRONMENT		5. FUNDING NUMBERS N6660495WR1132	
6. AUTHOR(S) Akira Tanaka			
7. PERFORMING ORGANIZATION NAME(S) AND ADDRESS(ES) Naval Postgraduate School Monterey CA 93943-5000		8. PERFORMING ORGANIZATION REPORT NUMBER	
9. SPONSORING/MONITORING AGENCY NAME(S) AND ADDRESS(ES) Naval Undersea Warfare Center New London Detatchment New London, CT 06320-5594		10. SPONSORING/MONITORING AGENCY REPORT NUMBER	
11. SUPPLEMENTARY NOTES The views expressed in this thesis are those of the author and do not reflect the official policy or position of the Department of Defense or the U.S. Government.			
12a. DISTRIBUTION/AVAILABILITY STATEMENT Approved for public release; distribution is unlimited.		12b. DISTRIBUTION CODE	

13. ABSTRACT

Energy spreading loss (ESL) is qualitatively defined as the reduction in peak echo level due to energy spreading of the transmitted acoustic pulse in time. An analysis of the impact of shallow water propagation on ESL was performed with the aid of a high performance computer using the FEPE_SYN and EXT_TD programs to compute the spreading of the received pulse due to multipath propagation in shallow water. A Blackman windowed pulse was used to model the transmitted pulse, which was centered at 3.5 kHz, with 200 Hz bandwidth. For input parameters, typical seasonal sound speed profiles and a Hamilton geoacoustic model of Area Foxtrot off the U.S. eastern seaboard was used. ESL's impact on sonar performance was determined as a function of range, source and target depth, sound speed profiles and geoacoustic properties. The impact of shallow water propagation on the correlation of the transmitted and propagated pulses through the quantitative definition of mismatch loss (MML) was also discussed.

The results showed that strong ESL (5 to 10 dB) existed over a sand (reflective) bottom and was generally invariant with range. ESL was correlated with TL, i.e., areas of high spreading loss were found in regions of high TL. ESL was not as large (3 to 5 dB) over silt/clay (absorptive) bottoms due to the increased absorption of the bottom refracted path thus reducing the number of multipath modes. Broadband pulses were found to exhibit fewer fluctuation than single frequency signals, and generally the total TL loss was a few dB larger than a single cw case. To overcome the ESL, integration techniques based on an accurate prediction model in the post analyzing system are required with a high temporal resolution of the echo energy shape.

14. SUBJECT TERMS Acoustics, Energy Spreading Loss, ESL, Underwater System, FEPE, FEPE_SYN, Broadband Analysis, Active Sonar, Hamilton Geoacoustic Model, Transmission Loss, Mismatch Loss, MML, Time Domain Analysis			15. NUMBER OF PAGES 102
			16. PRICE CODE
17. SECURITY CLASSIFICATION OF REPORT Unclassified	18. SECURITY CLASSIFICATION OF THIS PAGE Unclassified	19. SECURITY CLASSIFICATION OF ABSTRACT Unclassified	20. LIMITATION OF ABSTRACT UL

AN ANALYSIS OF ENERGY SPREADING LOSS ASSOCIATED WITH TACTICAL ACTIVE SONAR PERFORMANCE IN A SHALLOW WATER ENVIRONMENT

Akira Tanaka
Lieutenant Commander, Japanese Navy
B.S., National Defence Academy, Japan, 1982

Submitted in partial fulfillment
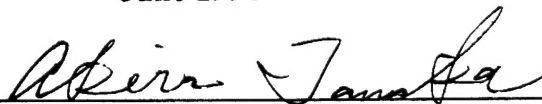of the requirements for the degree of

MASTER OF SCIENCE IN OCEANOGRAPHY
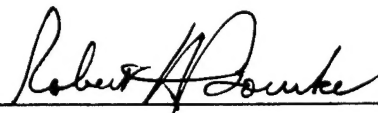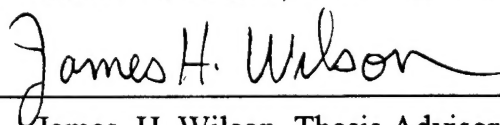
from the

NAVAL POSTGRADUATE SCHOOL
June 1996
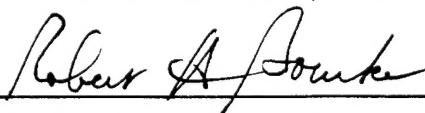
Author: _____

Akira Tanaka

Approved by: _____

Robert H. Bourke, Thesis Advisor

_____

James H. Wilson, Thesis Advisor

_____

Robert H. Bourke, Chairman, Department of Oceanography

iii

ABSTRACT

Energy spreading loss (ESL) is qualitatively defined as the reduction in peak echo level due to energy spreading of the transmitted acoustic pulse in time. An analysis of the impact of shallow water propagation on ESL was performed with the aid of a high performance computer using the FEPE_SYN and EXT_TD programs to compute the spreading of the received pulse due to multipath propagation in shallow water. A Blackman windowed pulse was used to model the transmitted pulse, which was centered at 3.5 kHz, with 200 Hz bandwidth. For input parameters, typical seasonal sound speed profiles and a Hamilton geoacoustic model of Area Foxtrot off the U.S. eastern seaboard was used. ESL's impact on sonar performance was determined as a function of range, source and target depth, sound speed profiles and geoacoustic properties. The impact of shallow water propagation on the correlation of the transmitted and propagated pulses through the quantitative definition of mismatch loss (MML) was also discussed.

The results showed that strong ESL (5 to 10 dB) existed over a sand (reflective) bottom and was generally invariant with range. ESL was correlated with TL, i.e., areas of high spreading loss were found in regions of high TL. ESL was not as large (3 to 5 dB) over silt/clay (absorptive) bottoms due to the increased absorption of the bottom refracted path thus reducing the number of multipath modes. Broadband pulses were found to exhibit fewer fluctuation than single frequency signals, and generally the total TL loss was a few dB larger than a single cw case. To overcome the ESL, integration techniques based on an accurate prediction model in the post analyzing system are required with a high temporal resolution of the echo energy shape.

TABLE OF CONTENTS

ACKNOWLEDGEMENTS

I. INTRODUCTION

A. NAVY'S INTEREST IN ASW

After the end of the cold-war the U.S. Navy's strategic interests shifted from deep water to shallow water issues because of the decrease of the threat of global war and the increased threat of regional conflicts. It is anticipated that these smaller scale conflicts will probably occur in littoral regions, not in the deep ocean. Since there is no longer a large foreign Navy to challenge the U.S. Navy on the open seas, regional conflicts, dominated by quiet diesel submarines and densely populated minefields, have become the USW challenge of the present.

The seas of littoral regions are usually shallow and their high spatial and temporal variability requires a high degree of knowledge of shallow water oceanography and acoustics to counter the ASW and mine warfare threats. Shallow water regions by definition are very complex oceanographically and acoustically due to temporal, spatial and spectral variations of environmental parameters.

Recent developments in sound silencing technology have resulted in submarines becoming very quiet, and advances in air injection propulsion (AIP) systems have made very long operation times on the battery possible. These improvements have increased the importance of active sonar operations in shallow waters. Accordingly, the assessment and improvement of

1

active sonar performance in shallow water is now a major concern to ASW planners and operators.

B.   BACKGROUND

Shallow water acoustics has long been a topic of ASW research but with emphasis on low frequency (< 1000 Hz) propagation [Urick, 1983]. Observations and model studies have shown that low frequency sound propagation in shallow water, especially for situations where the geoacoustic impact of the bottom/subbottom is significant [Hamilton, 1972, 1979, 1980, 1985, 1987; Jackson and Briggs, 1992; Hamilton and Bachman et al, 1982; Mourad and Jackson, 1983], is a complex problem. The complexity arises because many environmental acoustic parameters, such as the temperature and salinity of the water column, bathymetry, type of sediment, background noise, marine life, etc.., are highly variable, both temporally and spatially.

For tactical active sonar performance, the focus is on higher frequency sound propagation (order of several kHz), which is generally addressed in terms of ray acoustics. Ray acoustics is an accurate approximation to the full wave equation at high frequencies in deep water where diffraction effects are negligible. In shallow water diffraction and multipath interaction limit the use of ray acoustics and full wave solutions are required [Scanlon, 1995]. Although a full wave equation solution requires a significant computer

intensive effort at high frequencies, accurate approximations such as the Finite Element Parabolic Equation (FEPE) [Collins, 1988] exist to solve this problem and it is this model which has been selected for use in this analysis. FEPE is a single frequency (i.e., zero bandwidth) model for a continuous wave source. A time domain version of FEPE, called FEPE_SYN [Collins, 1989], is necessary to predict the time arrival structure of a pulse of finite bandwidth.

Because of the small range and depth steps required at the relatively high frequency of 3.5 kHz, the calculation of the full wave solution would have taken an astronomical length of time several years ago. Now computing power is available to realistically process time series data with modern powerful computers.

It is difficult to improve sonar performance in shallow water because of the phenomena of "Energy Time Spreading ." This phenomena has been known for more than 20 years [Bell, 1990] as it relates to low frequency passive acoustics, and was reported as time stretching due to "multipath effects". However, energy spreading loss (ESL) has not been widely modeled or measured as an active sonar equation parameter. Jensen (1993) and several NUSC researchers [Jones, 1990; Bell, 1990] have performed some excellent initial research on ESL for active acoustic sonar systems recently. Since their research efforts were based on observational data, no ESL modeling capability was available which attempted to solve the

3

full wave equation in the time domain.

In this research, ESL is treated as an active sonar equation parameter as an additional loss in addition to the standard terms. The models "FEPE_SYN" [Collins, 1989] and "EXT_TD" [Rovero, 1992] are used to estimate its magnitude and time spreading characteristics based upon an acoustic pulse of finite bandwidth transmitted from an active sonar system in shallow water. EXT_TD is used to add signal pulses of finite bandwidth to the time domain model FEPE_SYN.

1. Definition of ESL

Energy spreading loss (ESL) is defined qualitatively as the reduction in peak energy (or power) level due to the spreading of the energy of a transmitted acoustic pulse with time beyond the original transmitted pulse length. ESL is quantitatively defined in two ways: the first is the reduction in peak energy level to total energy [Jones, 1990]; the second is the coherence loss of a matched filter due to mismatching of the pulse shape [Jensen and Sabbadini, 1993]. The first energy-based definition of ESL is termed "ESL" while the second coherence measure is termed the "mismatch loss (MML)" to differentiate them physically.

ESL is based on the time stretching of the transmitted pulse, in which the pulse is stretched in time by multipath propagation. The time stretching causes the peak energy of the received pulse at a given point to be reduced below that of an echo at the same range but for which no multipath propagation

4

occurs, e.g., in deep water.

MML is based on the change in correlation or coherence between the transmitted and received pulse shapes at the receiver, a definition proposed by Jensen and Sabbadini (1993) for the deep bottom reflected case.

2. Past ESL Results

ESL has been studied over the past 20 years by a number of researchers as a multipath effect [Bell, 1990]. ESL is a complex phenomena of multipath or multimode wave propagation prevalent in shallow water. The term "energy splitting loss" was introduced by Stewart and Brandon (1967) to describe the type of signal distortion process whereby multipaths can split the echo energy into a number of resolvable arrivals.

"Energy spreading loss" was suggested by Weston (1965) who observed that the correlation loss due to spreading in the time delay was precisely the same phenomenon as the time spread and associated reduction in peak level observed when a short ping was transmitted.

The standard deviation, σ, of the stretched pulses in the time domain about the mean arrival time of the pulses has been used as a measure of time stretching and has been widely used in previous ESL studies [Van Trees, 1971]. The following equations summarize the use of the standard deviation as a

parameter to measure ESL:

$$\int \underline{A}^2(t)\,dt = \sum [s * A^2_{spread}(k)] = 1. \qquad (1-1)$$

$$\sigma = [\int (t-\mu)^2 \underline{A}^2(t)\,dt\,]^{1/2}$$
$$= \sum [(k*dt - \mu)^2 * s * A^2_{spread}(k)]^{1/2} \qquad (1-2)$$

$$\text{where} \quad \mu = \int t\,\underline{A}^2(t)\,dt = \sum [s * k*dt * A^2_{spread}(k)]\ . \qquad (1-3)$$

Here $\underline{A}^2$ represents normalized power, t represents time [sec], μ, the mean arrival time, $A^2_{spread}(k)$, the acoustic power at the k th time increment of the stretched pulse, k is the index number of the time increment and s is the normalization noise factor. Unfortunately, this measure of ESL was found to be corrupted by ambient noise in measurements of σ during at-sea experiments.

Bell (1990) modified Weston's definition of ESL by incorporating a Rayleigh distribution instead of a Gaussian distribution for the spread pulses. He used a Monte Carlo technique to include the effects of Rayleigh fluctuations in each resolvable part of the signal return. Bell's work was extended by Jones (1990) and his empirical equation (termed the "Bell-Jones Equation") gave good agreement with observed data [Chan, 1992]. Because the Bell-Jones equation related the

6

ratio of a time spreading function and system resolution, σ/R, to ESL, a threshold was set above a specified ambient noise level and a Gaussian distribution of the time spreading was assumed. Jones related the ratio of total energy (energy computed over the entire stretched signal) to peak energy (peak signal power times the resolution cell width) to ESL [Young, 1988],

$$ESL = 10*\log_{10}(TE / PE) \quad [dB].\qquad(1-4)$$

where TE represents the total energy and PE the peak energy. A resolution cell width, R, typically would be defined as the reciprocal of the correlator bandwidth BW [Hz].

$$R = 1 / BW \quad [sec].\qquad(1-5)$$

The ESL defined above is termed the "Jones ESL" in this study, which is used as a second measure of ESL.

Recently, Chan (1992) concluded that the multipath boundary interaction in the shallow water propagation channel accounted for most of the loss in expected performance of the wideband LPM (coded pulse) waveforms implemented on the AN/SQC-53C sonarset. The results indicated that ESL was a major loss mechanism in shallow water, and up to 12 dB of degradation was measured for specific waveforms. A modeling

7

technique which incorporated all frequencies in the signal band was used to model the time spreading in this experiment. Unfortunately, the model used is not considered to be accurate in shallow water.

Jensen and Sabbadini(1993) proposed MML (mismatch loss) as a measure of the signal degradation experienced by low frequency active (LFA) sonars. MML is based on the change of the peak pulse shape at the receiver compared to the shape of the transmitted pulse. The normalized coherence between the replica (transmitted) and a propagated pulse is given by,

$$\rho_{rp}(t) \;=\; \frac{\int V_r(t) * V_p(t-\tau)\ dt}{[\int V_r^2(t)\ dt]^{1/2} * [\int V_p^2(t)\ dt]^{1/2}} \qquad\qquad (1\text{-}6)$$

where Vr(t) is the replica pulse, Vp(t) is the propagated or received pulse near the maximum peak of the received pulse, and the interval for integration is usually taken as the duration of the replica pulse for matched filter processing [Jensen and Sabbadini, 1993]. MML is considered the third quantitative measure of ESL. Jensen and Sabbadini investigated LFA bottom bounce losses using a bottom interaction simulator and 1/100 scale cylinder-shaped target with rounded end caps. The bottom impulse response functions were obtained from SACLANT CENTER data. The experiment was

8

based on a bistatic geometry, and two bottom bounces for a pulse emitted at various launch angles, including 0, 45, 90 degrees of target aspect. Their results indicate that MML can reach 5.3 dB for a wideband (0.5 ~ 5 kHz), 1.5 sec LFM pulse (without target) in matched filter processing. Only under ideal (no spreading) conditions will LFA sonar performance predictions be realized when coherent processing is used.

In this study ESL and MML are calculated for one way propagation only (without the target) to focus the research on the impact of the environmental acoustic parameters affecting propagation on ESL/MML. A windowed Blackman pulse is used in all model runs to represent the outgoing pulse shape. This study will not address the impact of the transmitted wave pulse type, duration, etc., on ESL and MML.

The model results from this research are consistent with the measured ESL results of Chan (1992), where time spreading and energy spreading were the product of two way (monostatic) TL plus target scattering loss. It was not possible for Chan to analyze many pulses with exactly the same propagation environment since measured data (containing echo and reverberation) were used in his analysis, and thus he was forced to average different phased signals statistically. Similarly, Jensen and Sabbadini's analysis was limited because it did not account for multipath propagation, and therefore their MML was based on only one ray or predominant mode of the

9

acoustic wave.

3. Impact of ESL on Tactical Active Sonar Performance

Although ESL is generally incorporated as an additional loss term added in an ad hoc fashion to the active sonar equation, it is predicted by the wave equation. Without recognizing it, ESL has been measured as a part of TL in many past measurements [Urick, 1983] and is a major factor in total energy loss to the beamformer (excluding geometrical spreading) in shallow water. Whenever the wave equation is solved exactly, the solution includes ESL as well as TL if the model results are defined properly. Since the FEPE model solves the wave equation accurately, FEPE estimates ESL accurately. In this study a range independent environment is assumed that is invariant in time and the significant problems of sound speed fluctuations, sloping bottoms and spatially variable geoacoustic properties in shallow water are avoided.

For tactical active sonars, ESL can exert a significant degradation on sonar performance by reducing the detection range significantly in shallow water. This research demonstrates the impact of ESL degradation on active sonar performance as a function of source and target depth, range, sound speed profile and geoacoustic properties of the bottom.

Clearly TL is due to a geometrical spreading loss, absorption, and other boundary losses prior to the energy reaching the array. This energy can never be regained at the receiver location. However, it is possible to partially regain

10

ESL since the ESL energy arrives at the target location but is spread in time well beyond the original pulse width. This means it is possible to improve sonar performance if we can accurately model the spread of the transmitted pulses, and apply advanced beamforming/signal processing techniques such as Inverse Beamforming (IBF) [Nuttall and Wilson, 1991; Wilson, 1995; Fabre and Wilson, 1995].

In deep water the bottom boundary effects on propagation are relatively small and ESL is usually negligible at short range (< 15000 m). In shallow water where the bottom boundary effects are significant, ESL is large. Multipaths or multimodes generated by boundary interactions cause significant time stretching and result in large ESL. The physical description of time spreading which degrades sonar performance in shallow water is discussed in the next chapter.

C.   OBJECTIVE

This study attempts to define ESL quantitatively as a function of several parameters, e.g., range, source and target depth, water sound speed profile and composition of the sea floor. An analysis of the impact of shallow water propagation on ESL (based on this definition) is performed. The influence of ESL on sonar performance is discussed and recommendations are made to overcome the degradation due to ESL. An examination of the previous ESL definition [Jones, 1990] is also performed.

11

A second, but minor, objective is to analyze the impact of shallow water propagation on the correlation of the transmitted and propagated pulses through the quantitative definition of MML [Jensen and Sabbadini, 1993].

II. MODELING ESL IN SHALLOW WATER

A. SIGNAL PROPAGATION MODELS USED IN THIS ANALYSIS

1. FEPE_SYN and EXT_TD

FEPE_SYN is a fully range-dependent, time domain version of FEPE [Collins, 1989] in which the ocean transfer function (similar to TL) is calculated as the output. FEPE_SYN is implemented with a "window" in range and depth to limit the area over which the output is produced and a logfile is created which provides the structure of the data. FEPE_SYN was augumented by Rovero (1992) with a software program called EXT_TD to incorporate the propagation of finite length pulses with broadband responses and can easily be expanded to accommodate any new parameters required to match the transmitted pulse characteristics of existing tactical active sonars.

EXT_TD is a separate program which reads the output of FEPE_SYN and creates a time domain signal at a selected range and depth. A minor modification was made by the author to compare the resultant time spreading of the output pulse to the transmitted pulse length in order to calculate ESL values defined in the next section. As stated earlier, the source signal pulse shape used in this analysis is a Blackman windowed pulse.

Pulse propagation modeling is concerned with simulating the effects associated with the transmission of a finite

13

bandwidth signal characterized by a known frequency spectrum as contrasted with the more familiar single frequency continuous wave propagation. In principle, the frequency domain wave equation treats broadband signals by Fourier synthesis of individual cw solutions over the frequency spectrum. In the presence of nonlinearities, however, interaction among frequency components invalidates this frequency domain approach. In the time domain, the wave equation can be formulated using methods which remove pathological limitations from numerical solutions. [Etter, 1991]

Computers used in this research are the Power Onyx (2.75 MHz MIPS R8000CPUs, 64 bit operating system) Silicon Graphics Computer and the Model J916/4 Cray Computer, a powerful Cray research computer. It is impractical to obtain the ESL results without these, or even more powerful, computers at 3.5 kHz using a full wave propagation model such as FEPE_SYN.

2. Oceanographic/Geoacoustic Inputs

The input parameters were selected for a typical tactical sonar having a center frequency of 3.5 kHz, bandwidth of 200 Hz and at a depth of 7.3 m. An example of a typical FEPE_SYN input file is shown in Table 1. Oceanographic inputs were seasonal sound speed profiles and bathymetry profiles of Area Foxtrot, a tactical active sonar exercise area, south of Long Island. The geoacoustic inputs were a full Hamilton geoacoustic representation of sand and silt/clay sediment

14

types [Scanlon, 1995] found in Area Foxtrot.

3. FEPE

FEPE calculates the transmission loss only for a single frequency [Collins, 1989] and the latest version of FEPE was used to illustrate the TL as a function of range and depth in this study. Because ESL is strongly associated with TL (shown in Chapter V) and must be calculated separately from it, the FEPE TL results for a single frequency are used for comparison of TL from FEPE_SYN for the full 200 Hz signal bandwidth.

4. Strategy for Varying Input Parameters

For a frequency of 3.5 kHz, FEPE_SYN is very computer intensive. Sampling theory requires that a very small temporal increment be selected to avoid aliasing. The finite element method also requires a very small range and even smaller depth mesh size, to avoid spatial aliasing. In order to generate acoustic pulses with a maximum frequency of 3600 Hz, the Nyquist frequency of 7200 Hz is a minimum frequency limit for analysis. To be conservative, we chose a sampling rate of 4 * 3600 Hz = 16384 Hz to avoid aliasing. A 16,384 point FFT was used, producing a 1 Hz frequency resolution for a 1 sec time window.

The smallest wavelength in the transmitted pulse was used to determine the range/depth mesh for FEPE_SYN model runs.

$$c = \lambda * f \ , \ \text{or} \ \ \lambda = c/f \quad [m] \tag{2-1}$$

15

where c is sound speed [m/s], f is acoustic frequency [Hz] and λ is wavelength [m]. The maximum frequency and minimum sound speed determine the smallest λ. Therefore, the range/depth mesh was iteratively determined to be $dr = \lambda/2 = 0.206$ m and $dz = \lambda/10 = 0.041$ m, where fmax = 3600 Hz, c min = 1484 m/s for the data listed in Table 1.

This range/depth mesh makes the computational time tremendously long, and a typical model run takes more than 100 hours for the first of three phases of the computation. However, the objective of this research is to model energy spreading in the time domain, and measure TL and ESL quantitatively. Therefore, the long model run times are necessary and the development of a faster and more efficient program code is left for future research. The implementation of FEPE and FEPE_SYN on a massively parallel i860 array processor in a VMEbus is highly recommended for future ESL modeling computations at tactical sonar frequencies.

B. NEW QUANTITATIVE MEASURE OF ESL

Three measures to quantify ESL were introduced in the previous chapter (time spreading σ, Jones ESL and MML). Another measure of ESL is presented in this section and is based on the ability to model the time stretching of the signal accurately in shallow water.

ESL is the result of time stretching of the transmitted

16

pulse due to multipath propagation in shallow water. The peak energy of the received pulse is reduced due to this time spreading. To measure ESL, consider a pulse at some range from the source which has undergone no spreading and which is symmetric in amplitude about its peak value in the time domain. This idealized "no spread" pulse at range, r, has the same time duration as the transmitted pulse at range r = 1 m. The quantitative measure of ESL is based on the pulse source level or the total energy at 1 m from the source:

$$E_{replica} = \int_t^{t+\Delta t} A^2(t) \ dt = \sum A^2_{replica}(k) \qquad (2\text{-}2)$$

where E represents the total energy of the pulse, A represents the amplitude of the pulse at time t with a time increment dt and k is the number of time increments in the pulse, typically 16,384 in this study. $E_{replica}$ is used here to compare its magnitude to the received pulses.

In defining ESL quantitatively, an idealized, fictitious "no spread" pulse was determined by time compressing all of the pulse's time stretched energy into a pulse with no spreading that has the same pulse length and amplitude shape as the original transmitted Blackman pulse ($E_{replica}$).

Assuming that the shape of both the replica and the no spread pulses are symmetric in amplitude, the ratio is defined:

17

$$r = A_{nospread}(k) / A_{replica}(k) . \tag{2-3}$$

Since energy must be conserved at the target within the time window, for both the idealized "no spread" pulse and the actual time spread pulse, require

$$E_{nospread} = E_{spread} = \sum A^2_{spread}(k) . \tag{2-4}$$

Substituting Equations (2-2) and (2-3) into Equation (2-4) yields

$$E_{nospread} = \sum A^2_{nospread}(k) = r^2 * E_{replica} . \tag{2-5}$$

Thus, the factor r is given by:

$$r = (E_{nospread} / E_{replica})^{1/2} . \tag{2-6}$$

Therefore, one can obtain the peak value, $A_{nospread}{}^{max}(k)^2$ from the known values of $A_{replica}{}^{max}(k)^2$, $E_{replica}$ and E_{spread} as determined from Equation (2-4). Figure 1 shows the relationship of the peak values of the replica, no spread, and spread pulses. By defining these quantities as given by Equations (2-2) through (2-6) above, ESL and TL are automatically separated.

TL is the energy lost between the source and target and

18

is calculated by FEPE_SYN in the form:

$$TL = 10*\log_{10} (A_{nospread}{}^{max}/A_{replica}{}^{max})^2$$

$$+ 10*\log_{10} (R) \quad [dB] \tag{2-7}$$

where R is the range [m] from the source. ESL is the energy level that reaches the target that is spread in time beyond that of the original transmitted pulse length.

In order to determine how much energy is lost due to time spreading, the squared maximum amplitude of the spread pulse is compared to the squared maximum amplitude of the no spread pulse, and their ratio is defined as ESL:

$$ESL = 10*\log_{10} (A_{nospread}{}^{max} / A_{spread}{}^{max})^2$$

$$= 20*\log_{10} (A_{nospread}{}^{max} / A_{spread}{}^{max}) \quad [dB] \tag{2-8}$$

where $A_{nospread}{}^{max}$ is the absolute value of the peak amplitude (plus or minus) of the no spread pulse. $A_{spread}{}^{max}$ is the absolute value of the peak amplitude (plus or minus) of the largest time-stretched pulse.

A unique feature of the approach in this study is that the spread time series is modeled using very accurate, computer intensive models. Hence, no noise or artifacts contaminate this computation of ESL. Also, unlike previous studies, an assumed statistical distribution (e.g., Gaussian) for the time spread signal is not necessary; it is modeled

19

<u>directly</u>.

Table 1. Typical FEPE_SYN input data file

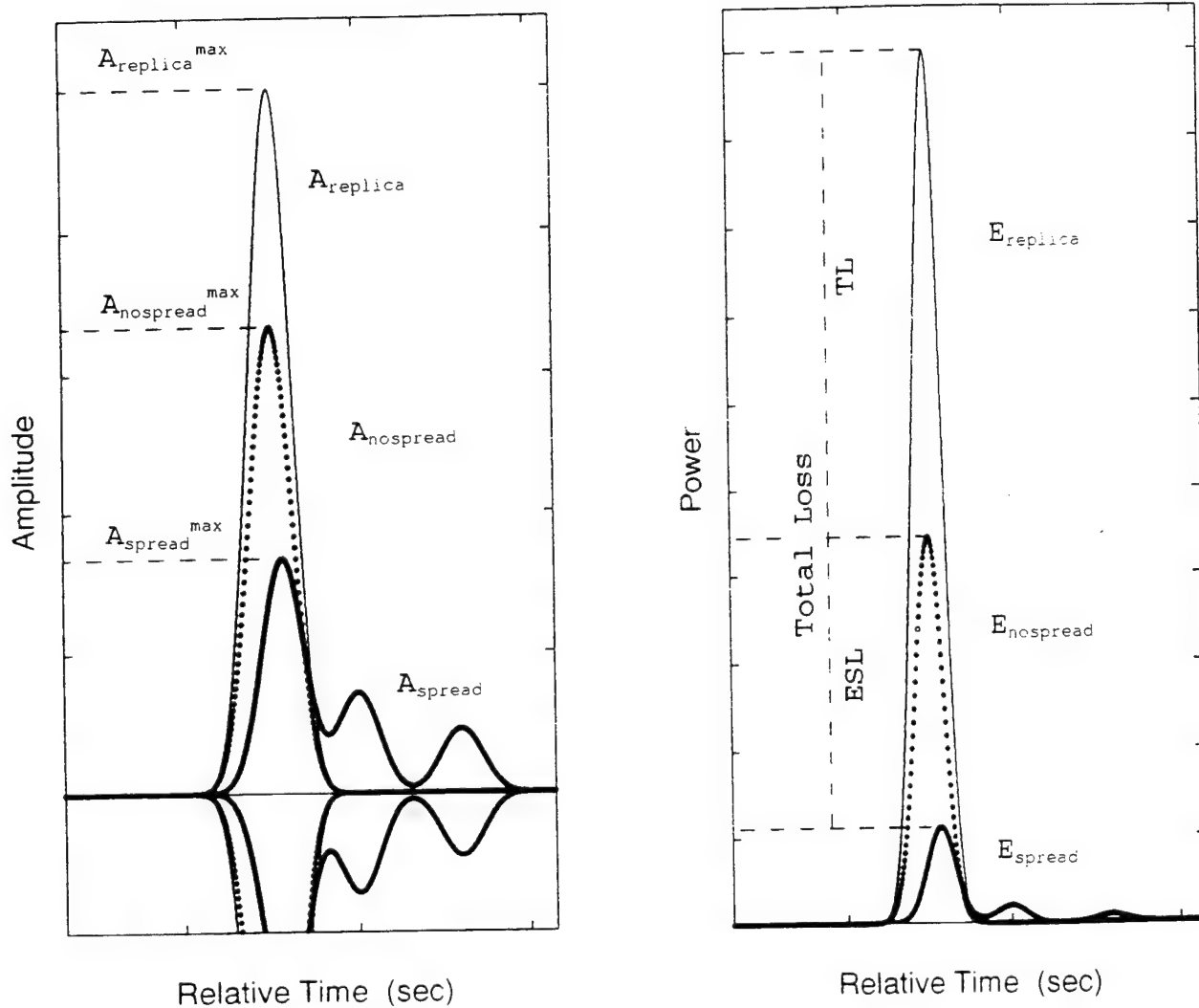| Input Variables	Comments
-200 800.0 .06103515 16384 3500.0 7.30 10.30555555 100 15000 15000 .206111111 50 110 .041222222 25 0.0 64.1 6000 1484.0 2 1 1.0 89.0	(TMIN, TMAX, DT, NDT) (FREQ, ZS, ZR) (RSTART, RFINISH) (RMAX, DR, NDR) (ZMAX, DZ, NDZ) (ZSTART, ZFINISH) (ISIZE) (C0, NPADE) (ISTRT, RMIN, THMAX) <Profile block (Hamilton geoacoustic model) follows as below>

0.000E+00   64.1
-1.000   -1.000
   *   *
   *   *
-1.000   -1.000
   *   *
   *   *
-1.000   -1.000
   *   *
   *   *
-1.000   -1.000
   *   *
   *   *
-1.000   -1.000
	(RD, D)
	
	(Z, CW)
	
	(Z, CB)
	
	(Z, RHOB)
	
	(Z, ATTN)
	
	<can repeat more profile blocks to model a range dependent model>

Figure 1. Relationship of the replica, no spread and spread pulses. Left: Amplitude of the pulses in the time domain. Right: Power (or acoustic energy) of the pulses in the time domain.

III. MODEL RESULTS

A. BACKGROUND

The transmitted pulse used in this study is a Blackman windowed pulse centered at 3500 Hz with a 200 Hz bandwidth, as shown in Figure 2. The Blackman pulse in the time domain is modeled with a pulse duration of 0.02 sec or 20 msec and is approximated by the FFT subroutine in EXT_TD. The received pulses are the Fourier synthesized time domain products of 200 transmitted single frequency signals, each subject to an ocean transfer function (similar to TL). Typical examples illustrating varying degrees of time stretching for a negative sound speed profile, overlying a sand bottom are shown in Figures 3 through 5. Figure 3 represents a situation with limited time stretching (ESL = 1 ~ 2 dB), Figure 4 moderate time stretching (ESL = 3 ~ 5 dB) and Figure 5 extensive spreading (ESL = 9 ~ 11 dB).

Four SSPs were used to determine the nature of ESL under widely varying, but common, shallow water SSPs (Figure 6). Here the negative type SSP (negative SSP) corresponds to the observational data of Area Foxtrot [Scanlon, 1995]. The isothermal type (isothermal SSP) represents well mixed conditions often found in winter in shallow water regions. The mixed layer type SSP (ML-type SSP) is representative of summer conditions where the water column has been warmed by

23

insolation but its upper portion has been mixed by wind forcing. The deep sea sound channel type SSP (SC-type SSP) is introduced to represent a typical deep water situation where little time stretching is anticipated at short ranges for a shallow source. Because of the extensive computer time required to perform the analysis for a typical 4000 m deep water column, the lower positive gradient of this profile has been increased to mimic deep water refraction patterns.

In order to examine the impact of a slow speed sediment bottom on ESL, the isothermal profile was arbitrarily increased by 70 m/sec ((b) in the upper right panel of Figure 6) to artificially create a slow speed sediment interface (slow speed SSP). Hamilton geoacoustic models for both sand and silt/clay bottoms were used as inputs to FEPE (Tables 2 and 3). These geoacoustic models correspond closely with the measured geological data in Area Foxtrot [Scanlon, 1995].

Because it is impractical to make three dimensional color plots for a pulse centered at 3.5 kHz with a 200 Hz bandwidth, two dimensional color plots at a single frequency, calculated by FEPE, are shown to illustrate propagation characteristics in shallow water. The horizontal and vertical resolution are 10.31 m and 0.21 m, respectively, for all the FEPE TL color plots. Figures 7 and 8 depict the TL for a negative SSP overlying a sandy bottom and a clay/silt bottom, respectively. A comparison of these two figures illustrates the impact of sediment type on TL. Because of the high attenuation

24

associated with a silt/clay bottom, the TL is significantly greater than for a sand bottom. Figure 9 is a plot of the TL for an isothermal (weakly positive) SSP overlying a sand bottom, and Figure 10 is a plot of TL for a mixed layer type (ML-type) SSP, sand bottom showing the favorable propagation conditions within the ML.

Figure 11 is an enlarged view of the TL shown in Figure 8 for the negative SSP silt/clay bottom case but for frequencies of 3400 Hz and 3600 Hz, the minimum and maximum frequencies within the bandwidth. The dispersion of acoustic energy over the 200 Hz bandwidth is readily noted. A difference of up to a 100 m is observed where the bottom bounce rays reflect from the bottom near 5000 m range. When modeling broadband pulses, TL computed by FEPE can only be considered a gross approximation to the propagation of finite bandwidth pulses because of this dispersion effect, but it can illustrate general TL properties for various environmental effects (e.g., SSP, sediment types, etc.) at the center frequency of the transmitted pulse. However, it is important to realize that FEPE TL estimates are for a single frequency only, with no temporal information about the pulse distribution, so that it can not be used to estimate ESL from a 200 Hz band sonar.

The ESL plots in the following sections were generated on workstation (UNIX) computers using MATLAB programs based on the definitions in the Chapter II. These MATLAB programs,

25

developed by the author, use the Cray/Onyx computer outputs of the time-stretched signal and calculate and display ESL based on Equation (2-8).

B.   RANGE DEPENDENCE OF ESL

Figure 12 shows ESL as a function of range between 0.1 km and 7.6 km for a negative SSP over a sand bottom. This plot has a range resolution of 10.3 m and ESL is plotted for targets positioned at 10.3 m depth intervals, i.e., from 10.3 m to 61.8 m. The range dependence of ESL for the transmitted pulse is not a linear function of range as might intuitively be expected, i.e., greater ranges would imply more time stretching of the pulse. However, as Figure 12 shows, ESL increases significantly for ranges from 0 m to 1600 m, but remains relatively constant at longer distances as the transmitted pulse begins to saturate in its interaction with the shallow water boundaries. As the energy propagates farther in range, the higher order normal modes begin to separate from the lower normal modes due to their different group speeds. However, the higher order mode energy (steeper ray equivalent angles) is continually attenuated at a relatively faster rate due to bottom boundary interactions. Beyond 1600 m most of the energy is carried by the lower order modes with little variation in group speed. Hence, the ESL remains fairly constant over this distance. This plot also demonstrates how ESL varies with depth of the target. ESL remains relatively

26

high at all depths (up to a maximum of 11 dB) over this entire range band, but is higher in the mid-depths (20.6 m to 41.2 m) due to the interference pattern of the different normal modes. Table 4 presents the mean and standard deviation of ESL for each depth over the range band 2000 m to 14500 m calculated at 10.31 m intervals. Over this range band the mean ESL varies from approximately 6.5 to 7.5 dB with a standard deviation of about 1.5 dB.

C.   DEPTH DEPENDENCE OF ESL

A plot of ESL versus depth is shown in Figure 13, which is based on a negative SSP over a sand bottom. These plots, based on a 1.031 m vertical resolution, pictorially describe how ESL varies throughout the water column at the ranges indicated above the individual panels (approximately 1000 m intervals). A weak depth dependence of ESL for depths above 15 m is noted due to the location of the source at 7.3 m. ESL is lower by 5 dB or more in the upper 15 m at selected ranges where the downward refracted energy from the shallow source returns to the near surface. In general, ESL is relatively independent of depth as noted in the previous section. Both high and low frequency fluctuations of 1 to 3 dB amplitude occur throughout the water column. For this source/SSP configuration strong high frequency fluctuations (1 to 6 dB) are observed between 20 m and 40 m.

The near constancy of ESL with depth is a result of the

27

coherent summation of approximately 290 to 307 modes propagating at different angles and at different group speeds at each frequency in the 200 Hz-wide band. Although higher order modes are attenuated faster, the interference pattern of the remaining modes results in smoothing the energy distribution throughout the water column. The fluctuations represent specific depth/range positions where constructive or destructive interference occurs.

This relative lack of depth dependence for ESL appears to be fairly universal as investigations were done for a variety of SSP shapes and bottom sediment conditions (discussed later) and all cases appeared to support this finding.

D. GEOACOUSTIC DEPENDENCE OF ESL

Significant changes occur in TL when the geoacoustic parameters and sediment properties exhibit high spatial variability in shallow water environments [Scanlon,1995]. For a location where the sediment compressional sound speed decreases due to the bottom transitioning from sand to silt/clay, one expects the received pulses to become fewer in number and show a significantly increased TL. Figure 14 shows ESL vs depth plots, for the isothermal SSP overlying a silt/clay bottom sediment. However, to model a "slow speed bottom", as described previously, the SSP in the water column has artificially been increased by 70 m/sec to create a low speed sedimentary layer. Because of the highly absorptive

28

nature of this slow speed bottom, only a few low order modes of similar group speed dominate the water column. Hence the number of time stretched pulses is expected to decrease. Only one pulse was observed for this case compared to 10 or more for the same SSP overlying a sand bottom. As seen in Figure 14, there is virtually no ESL observed at any range or depth.

As the bottom becomes more reflective, the amount of ESL is expected to increase. This is borne out by Figures 15 and 16 which show ESL vs depth plots, for an isothermal SSP overlying a silt/clay and a sand bottom, respectively. Comparing Figure 14 (slow speed bottom), Figure 15 (clay) and Figure 16 (sand), mean ESLs averaged over the depth of the water column are seen to increase from 0.1 dB, 2.7 dB, 6.5 dB, respectively. Although these relative changes in ESL were based on the slightly positive isothermal SSP, the dependence of the water column SSP is relatively weak as similar ESL values were obtained when a negative SSP was substituted. This dependence of ESL on the water column SSP is examined in further detail below.

E.   SSP DEPENDENCE OF ESL

The influence of the shape of the SSP of the water column on ESL can be examined by varying the SSP but keeping the geoacoustic properties of the bottom constant. Three SSPs were considered: the ML-type SSP (Figure 17), the negative SSP (Figure 13) and the isothermal SSP (Figure 16), all overlying

29

a sand bottom. The ML-type SSP is essentially a combination of the isothermal and the negative SSP. As can be seen in Figure 17, ESL remains moderately low (~ 6.5 dB) in the mixed layer, but becomes larger (~ 9 dB) below the mixed layer (ML) with large scale fluctuations (2 ~ 3 dB) frequently occuring. In fact, these below layer ESL values were the highest encountered of all SSP/bottom type configurations examined. For the negative SSP (Figure 13), acoustic energy is forced towards the bottom, so that ESL becomes large (average of 7.0 dB for each depth column beyond 5152 m). For the isothermal SSP (Figure 16), acoustic energy is forced upward weakly, minimizing the amount of energy which penetrates into the bottom. For the reflective sand bottom a relatively moderate ESL is observed (~ 6.5 dB) for ranges beyond 5152 m.

These three examples demonstrate that the shape of the water column SSP exerts a relatively insignificant influence on ESL. For the reflective bottom type considered, all three yielded nearly similar values (7 ~ 8 dB). Negative SSPs cause ESL values to be slightly greater (~ 1 dB) than upward refracting SSPs. This variability is small compared to the 3 ~ 5 dB difference noted between an absorptive (silty) and reflective (sandy) bottom.

Because the SSP shape has only a limited effect on ESL, this suggests there will be only a limited seasonal

30

variability associated with ESL for any given shallow water
location.

Table 2. A Hamilton geoacoustic model for a sand bottom in Area Foxtrot

depth

water column sound speed (m/s):

depth	value
0.000000E+00	1519.000
6.250000	1518.000
12.50000	1516.000
18.75000	1512.000
25.00000	1509.000
31.25000	1506.000
37.50000	1500.000
43.75000	1496.000
50.00000	1493.000
56.25000	1490.000
62.50000	1488.000
64.00000	1484.000
64.10000	1484.000
-1.000000	-1.000000

compressional wave speed (m/s):

depth	value
64.10000	1817.000
65.00000	1934.400
66.00000	1934.850
67.00000	1935.290
68.00000	1935.720
69.00000	1936.140
70.00000	1936.560
71.00000	1936.970
72.00000	1937.380
73.00000	1937.780
74.00000	1938.180
75.00000	1938.570
76.00000	1938.950
77.00000	1939.330
78.00000	1939.710
79.00000	1940.080
80.00000	1940.440
81.00000	1940.810
82.00000	1941.000
83.00000	1941.520
84.00000	1941.870
85.00000	1942.210
86.00000	1942.550
87.00000	1942.890
88.00000	1943.220
89.00000	1943.550
90.00000	1943.880
91.00000	1944.200
92.00000	1944.520
93.00000	1944.830
94.00000	1945.140
94.10000	2000.000
110.0000	2000.000
-1.000000	-1.000000

sediment density (g/cm^3):

depth	value
64.10000	2.600000
65.00000	2.600000
66.00000	2.600000
67.00000	2.610000
68.00000	2.610000
69.00000	2.620000
70.00000	2.620000
71.00000	2.630000
72.00000	2.630000
73.00000	2.640000
74.00000	2.640000
75.00000	2.650000
76.00000	2.650000
77.00000	2.650000
78.00000	2.660000
79.00000	2.660000
80.00000	2.670000
81.00000	2.670000
82.00000	2.680000
83.00000	2.680000
84.00000	2.690000
85.00000	2.690000
86.00000	2.720000
87.00000	2.740000
88.00000	2.760000
89.00000	2.780000
90.00000	2.800000
91.00000	2.810000
92.00000	2.820000
93.00000	2.830000
94.00000	2.840000
94.10000	2.850000
110.0000	2.850000
1.000000	-1.000000

sediment attenuation (dB/λ):

depth	value
64.10000	0.7034740
65.00000	0.8056971
66.00000	0.8307893
67.00000	0.8309792
68.00000	0.8311670
69.00000	0.8313505
70.00000	0.8315299
71.00000	0.8317071
72.00000	0.8318844
73.00000	0.8320595
74.00000	0.8322304
75.00000	0.8323971
76.00000	0.8325637
77.00000	0.8327284
78.00000	0.8328909
79.00000	0.8330534
80.00000	0.8332115
81.00000	0.8333656
82.00000	0.8335091
83.00000	0.8336610
84.00000	0.8338214
85.00000	0.8339733
86.00000	0.8341210
87.00000	0.8342644
88.00000	0.8344080
89.00000	0.8345492
90.00000	0.8346906
91.00000	0.8348320
92.00000	0.8349692
93.00000	0.8351042
94.00000	0.8352392
94.10000	0.8396534
110.0000	20.00000
1.000000	-1.000000

Table 3. A Hamilton geoacoustic model for a silt/clay bottom in Area Foxtrot

depth — water column sound speed (m/s)

depth	sound speed
0.000000E+00	1519.000
6.250000	1518.000
12.50000	1516.000
18.75000	1512.000
25.00000	1509.000
31.25000	1506.000
37.50000	1500.000
43.75000	1496.000
50.00000	1493.000
56.25000	1490.000
62.50000	1488.000
64.00000	1484.000
64.10000	1484.000
-1.000000	-1.000000

compressional wave speed (m/s)

depth	wave speed
64.10000	1550.000
65.00000	1550.500
66.00000	1555.000
67.00000	1560.000
68.00000	1565.000
69.00000	1570.000
70.00000	1580.100
71.00000	1584.000
72.00000	1587.300
73.00000	1590.300
74.00000	1593.000
75.00000	1595.400
76.00000	1597.600
77.00000	1599.700
78.00000	1601.600
79.00000	1603.300
80.00000	1605.000
81.00000	1606.500
82.00000	1608.000
83.00000	1609.400
84.00000	1610.700
85.00000	1611.900
86.00000	1613.100
87.00000	1614.300
88.00000	1615.400
89.00000	1616.400
90.00000	1617.400
91.00000	1618.400
92.00000	1619.400
93.00000	1620.300
94.00000	1621.100
94.10000	1621.200
110.0000	1632.200
-1.000000	-1.000000

sediment density (g/cm^3)

depth	density
64.10000	1.500000
65.00000	1.500000
66.00000	1.500000
67.00000	1.510000
68.00000	1.510000
69.00000	1.520000
70.00000	1.520000
71.00000	1.530000
72.00000	1.530000
73.00000	1.540000
74.00000	1.540000
75.00000	1.550000
76.00000	1.550000
77.00000	1.550000
78.00000	1.560000
79.00000	1.560000
80.00000	1.570000
81.00000	1.570000
82.00000	1.580000
83.00000	1.580000
84.00000	1.590000
85.00000	1.590000
86.00000	1.620000
87.00000	1.640000
88.00000	1.660000
89.00000	1.680000
90.00000	1.700000
91.00000	1.710000
92.00000	1.720000
93.00000	1.730000
94.00000	1.740000
94.10000	1.750000
110.0000	1.750000
-1.000000	-1.000000

sediment attenuation (dB/λ)

depth	attenuation
64.10000	0.400000
65.00000	0.410000
66.00000	0.420000
67.00000	0.430000
68.00000	0.440000
69.00000	0.450000
70.00000	0.460000
71.00000	0.470000
72.00000	0.480000
73.00000	0.490000
74.00000	0.500000
75.00000	0.510000
76.00000	0.520000
77.00000	0.530000
78.00000	0.540000
79.00000	0.550000
80.00000	0.560000
81.00000	0.570000
82.00000	0.580000
83.00000	0.590000
84.00000	0.600000
85.00000	0.610000
86.00000	0.620000
87.00000	0.630000
88.00000	0.640000
89.00000	0.650000
90.00000	0.660000
91.00000	0.670000
92.00000	0.680000
93.00000	0.690000
94.00000	0.700000
94.10000	0.710000
110.0000	20.00000
-1.000000	-1.000000

Table 4. The mean and standard deviation of ESL

Depth(m)	Mean ESL(dB)	Std ESL(dB)
10.3	5.0364	1.712
20.6	6.9412	1.474
30.9	7.2397	1.466
41.2	7.6396	1.429
51.5	6.7190	1.210
61.8	5.9725	1.171
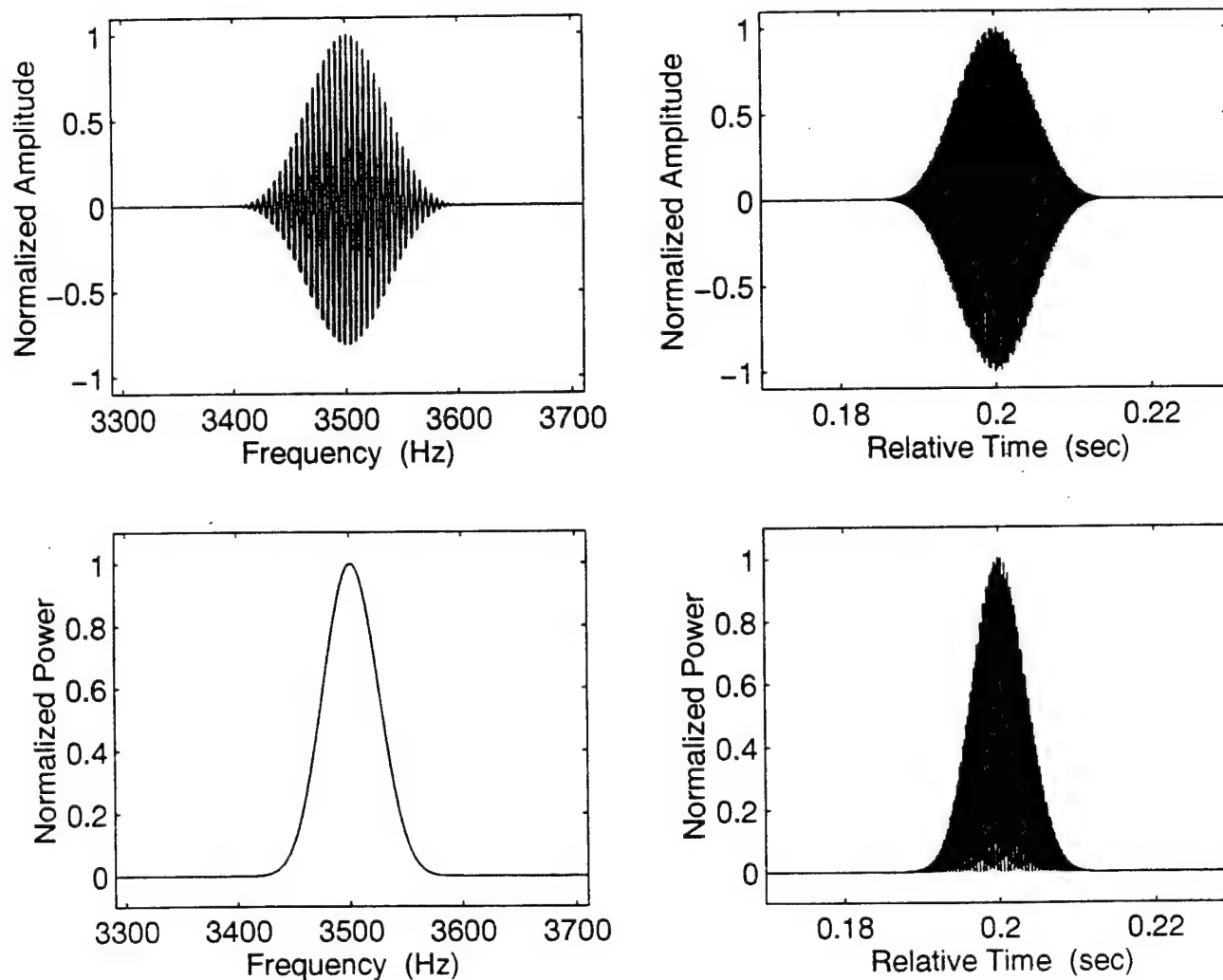
Figure 2. A Blackman windowed pulse, used as the input
transmitted pulse in this research, is shown in the
frequency domain (left) and in the time domain (right). The
upper panels are the amplitudes normalized by the peaks;
the lower panels are the power (or acoustic energy)
normalized by the peaks.

35
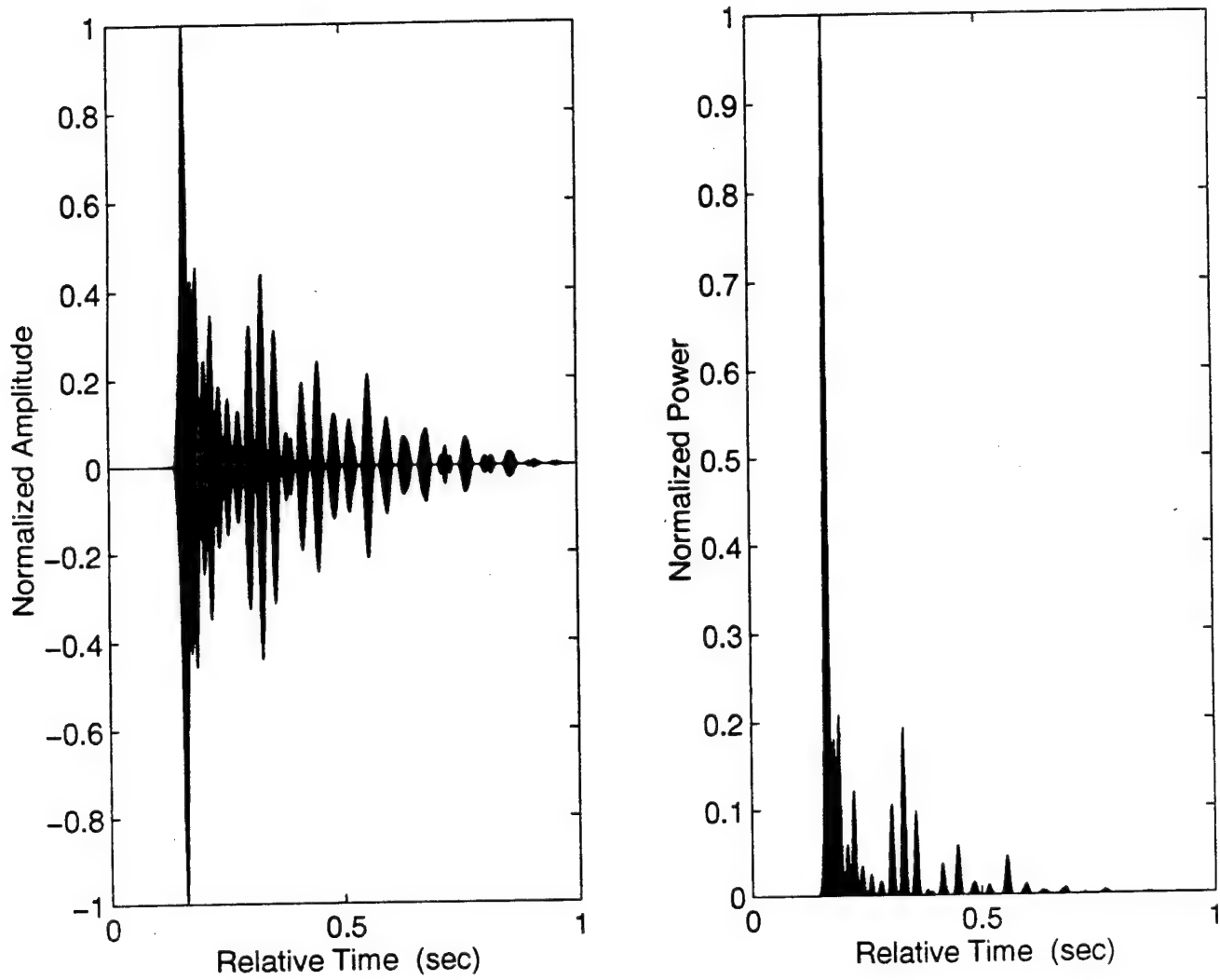
Figure 3. An example of time stretching illustrating low
ESL (~ 2 dB) for a negative SSP overlying a sand bottom;
source depth is 7.3 m.
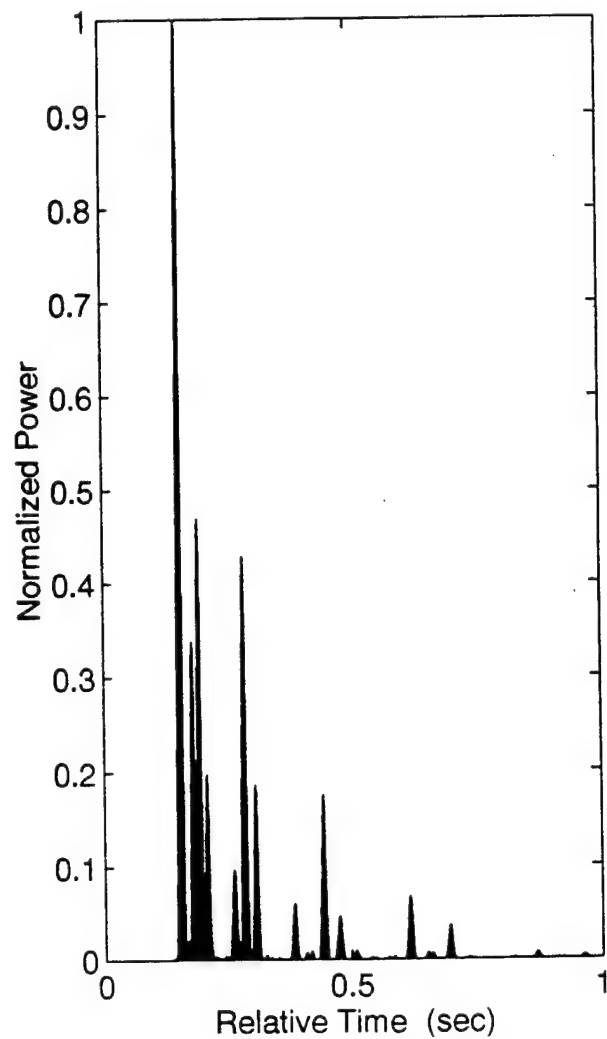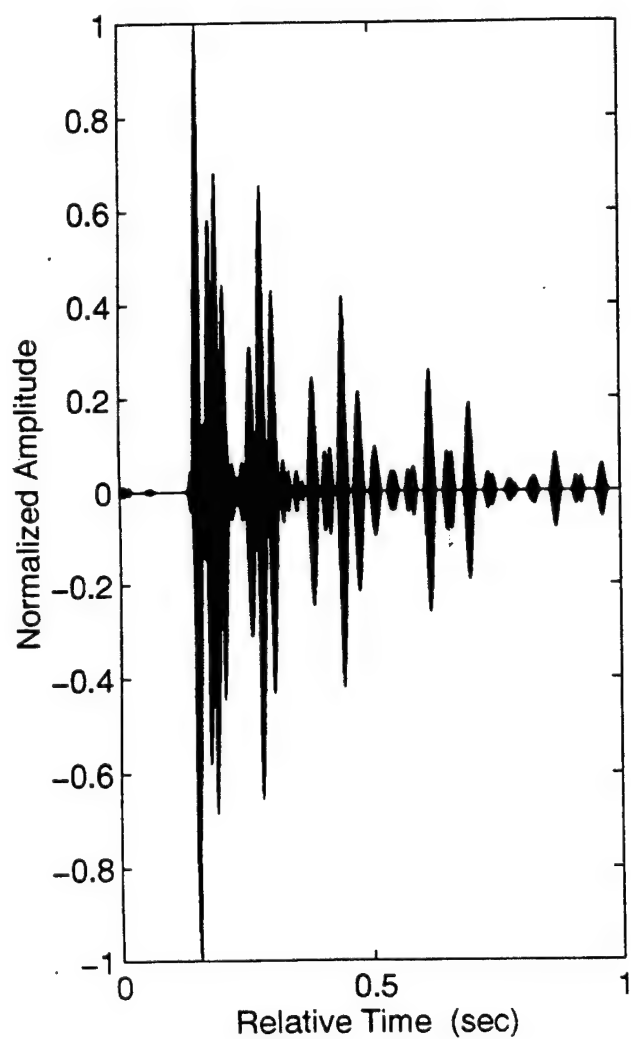
Figure 4. Same as Figure 3 except illustrating moderate ESL
(~ 4 dB).
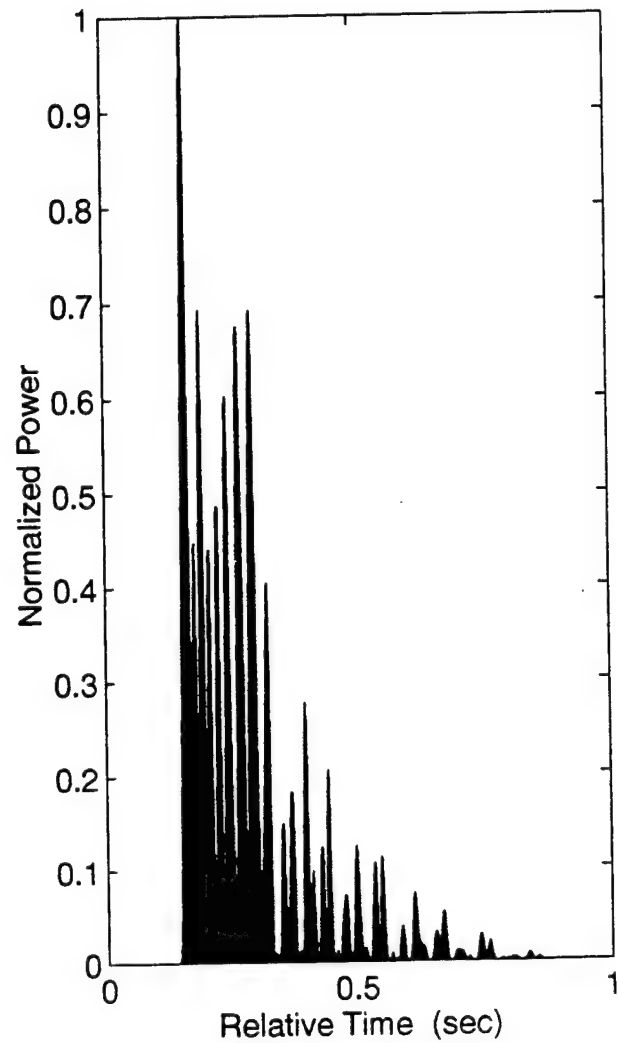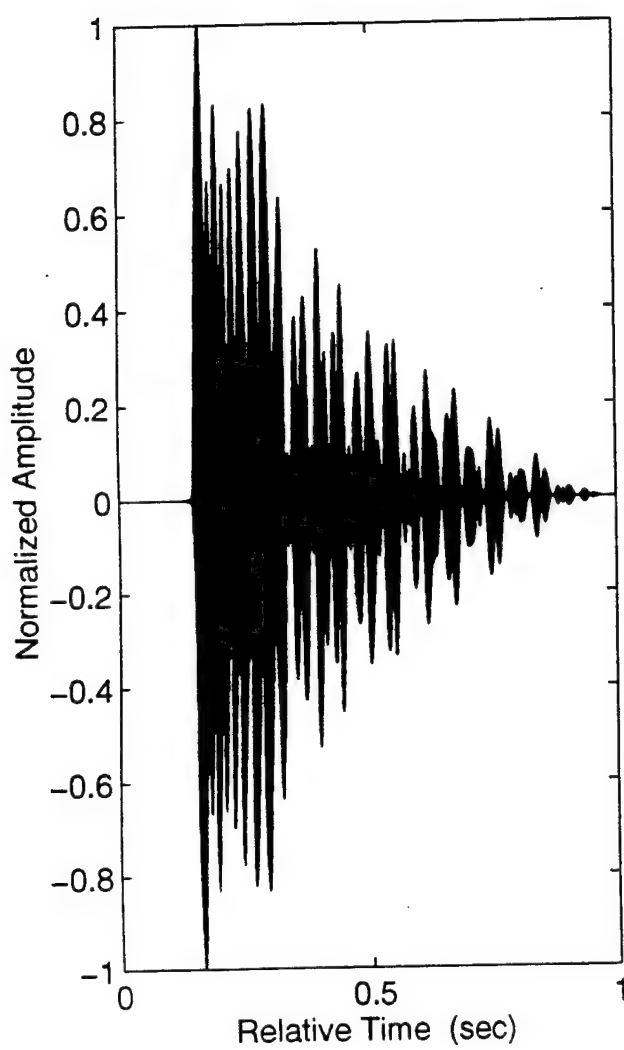
Figure 5. Same as Figure 3 except illustrating large ESL (~ 10 dB).
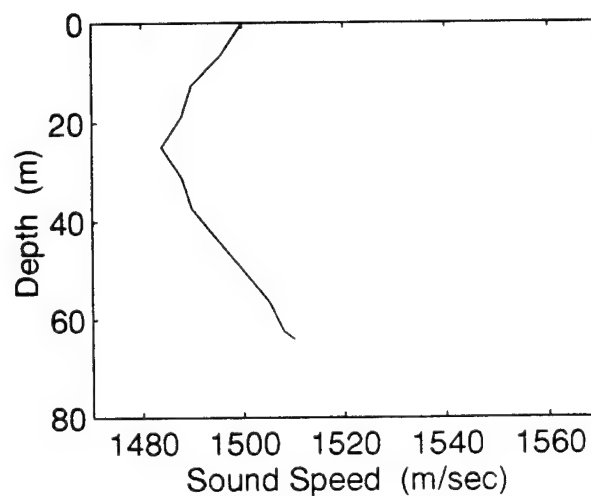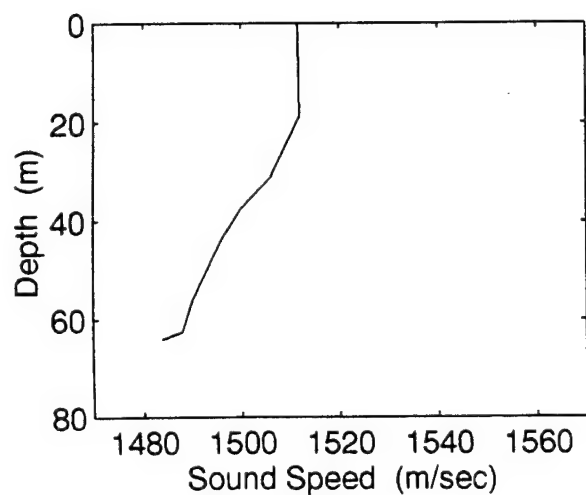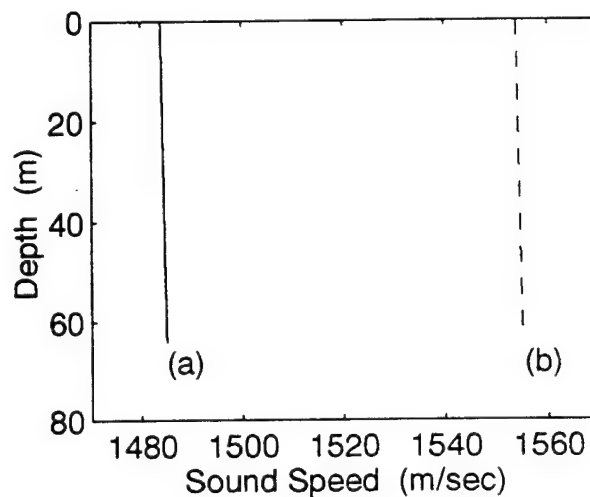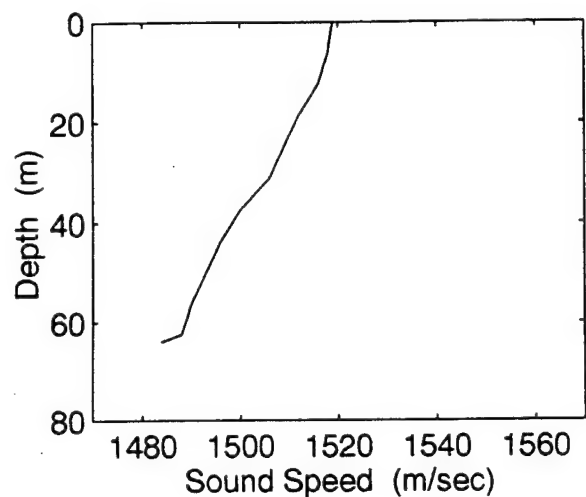
Figure 6. Sound speed profiles (SSP) used in this research: "negative SSP" (upper left), "isothermal SSP" (upper right), "mixed layer(ML)-type SSP" (lower left), "sound channel(SC)-type SSP" (lower right).
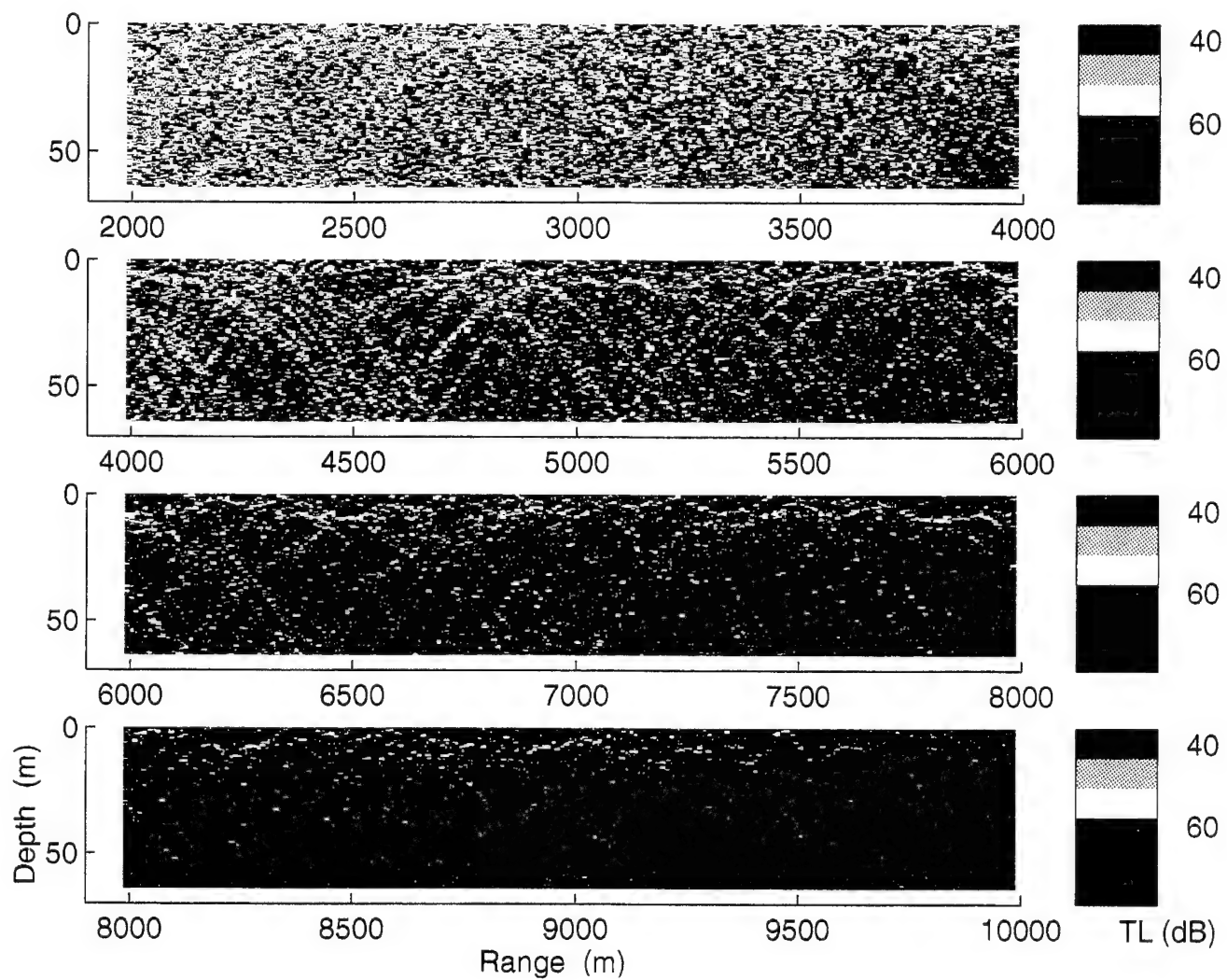
Figure 7. Three dimensional TL plots by FEPE for 3.5 kHz
(single frequency), for a negative SSP overlying a sand
bottom; water depth is 64 m, source depth is 7.3 m.

40
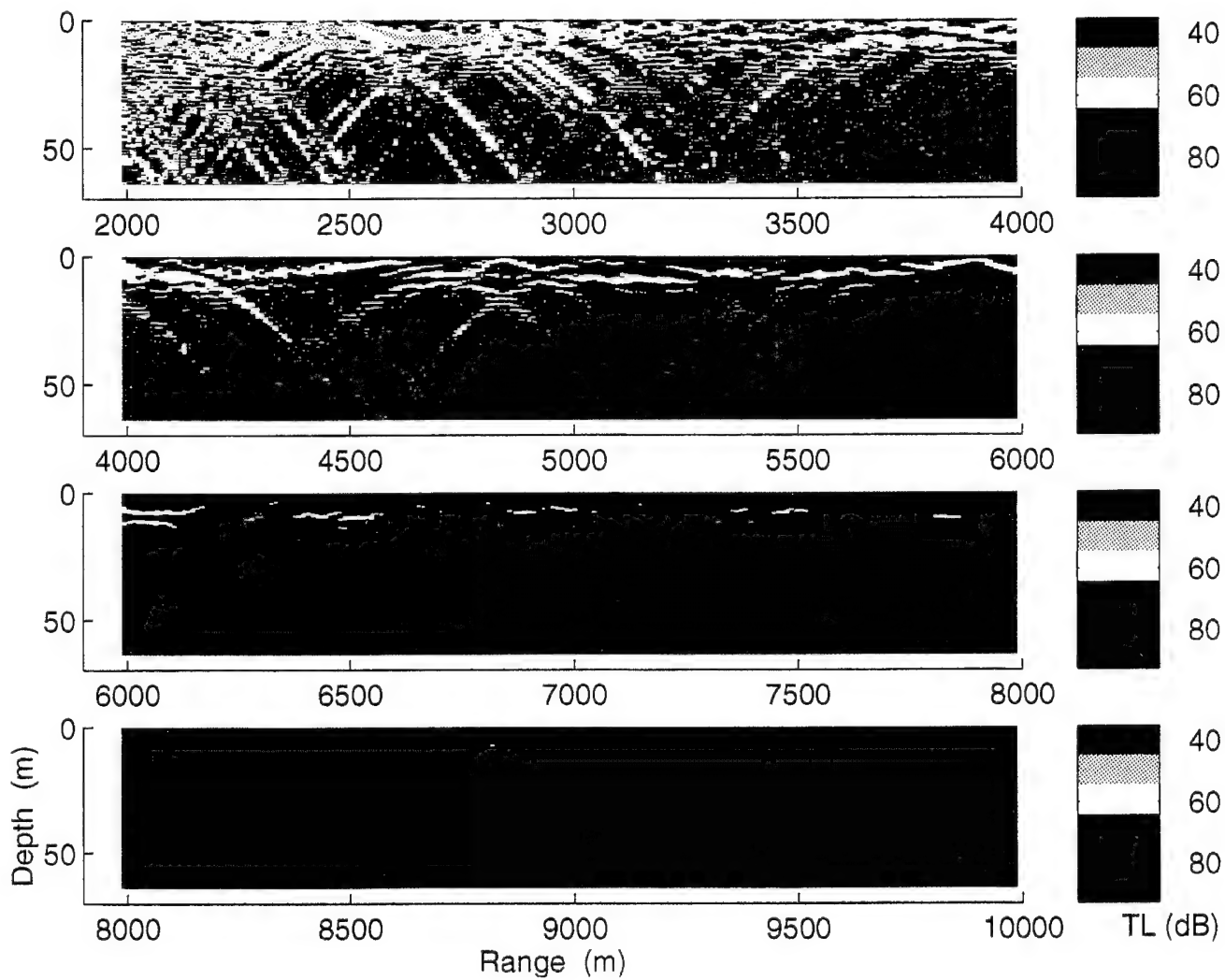
Figure 8. Same as Figure 7 except for a silt/clay bottom. The color bar scale was changed due to large TL for this case.
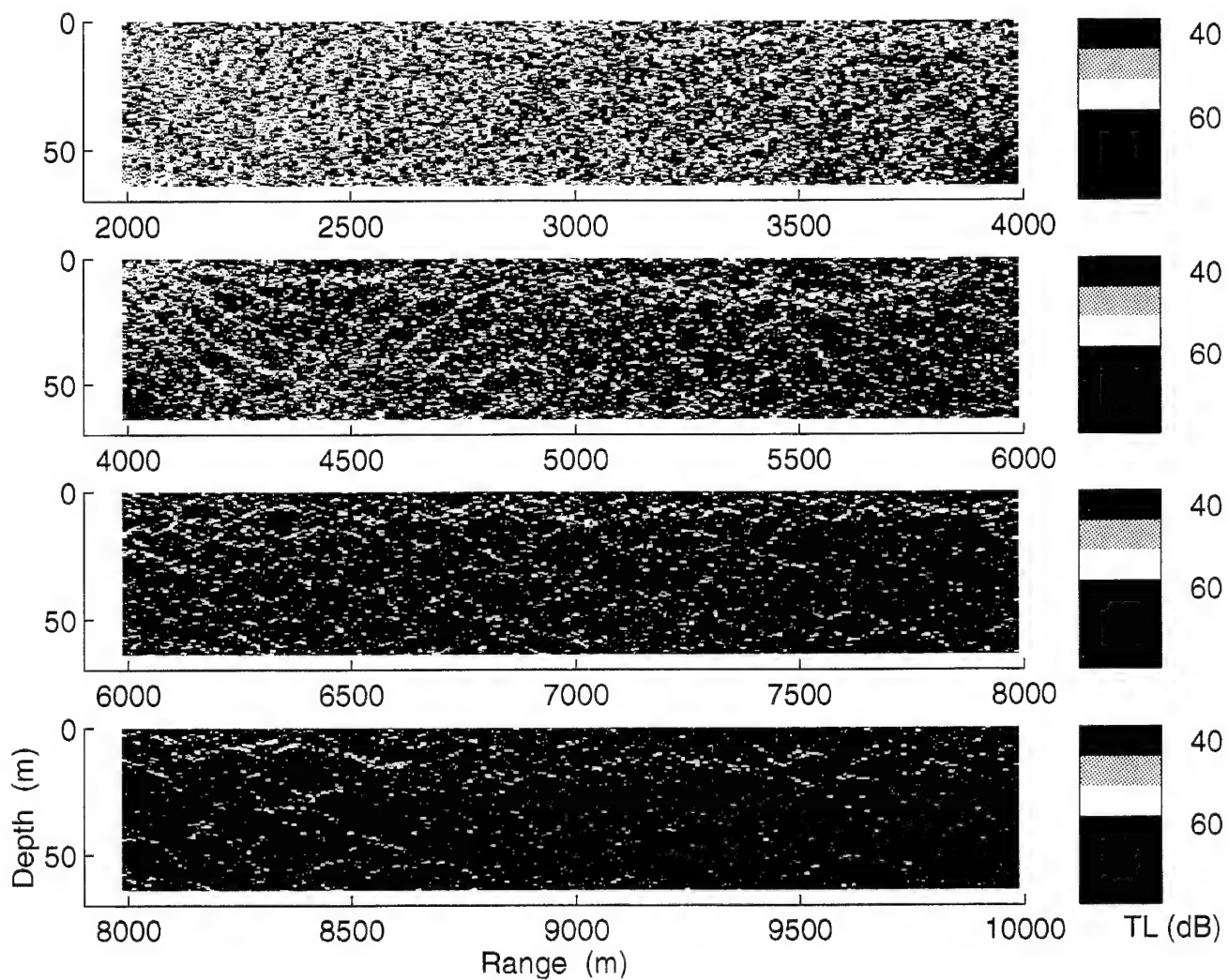
Figure 9. Same as Figure 7 except an isothermal SSP is used.
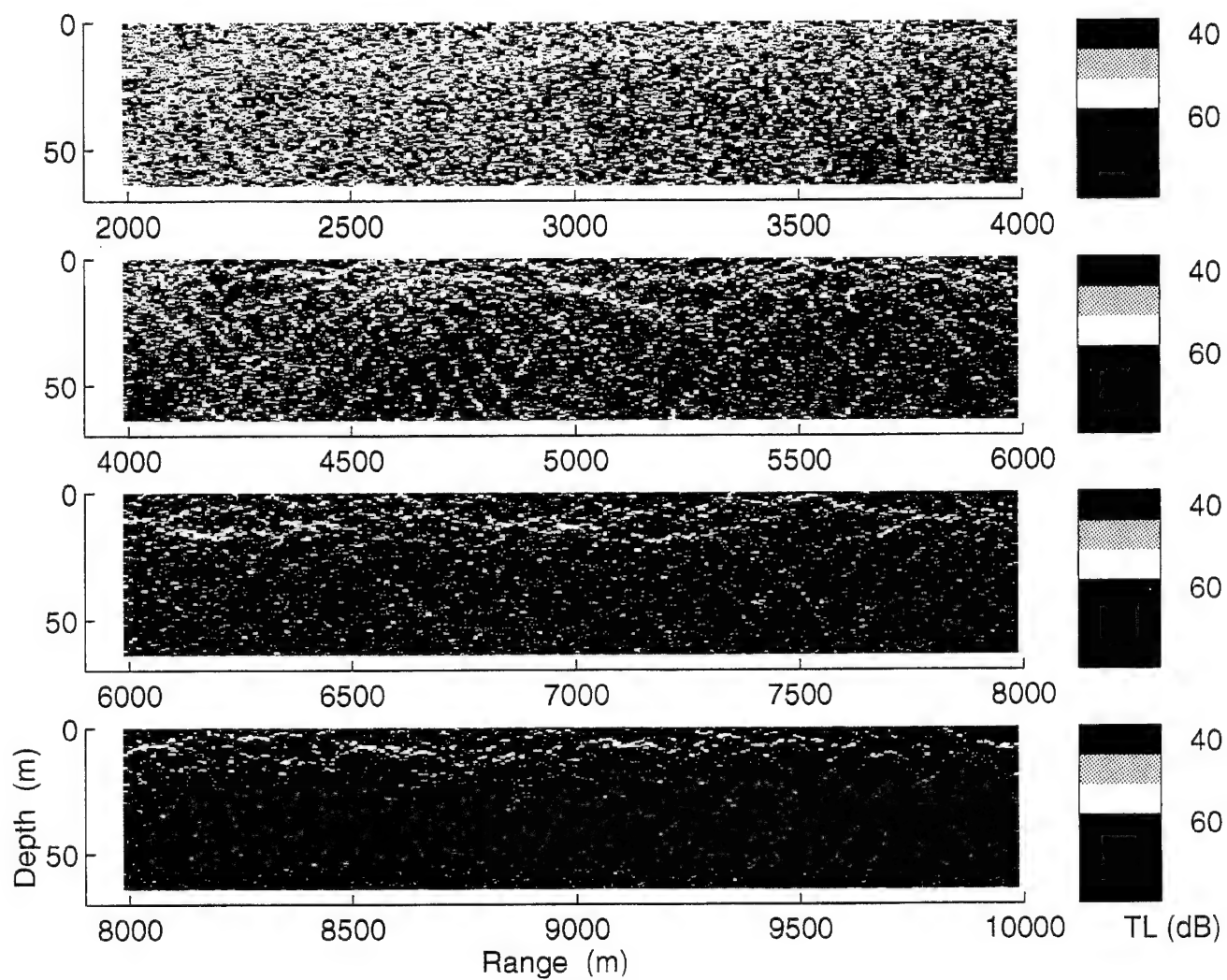
Figure 10. Same as Figure 7 except a mixed layer type SSP
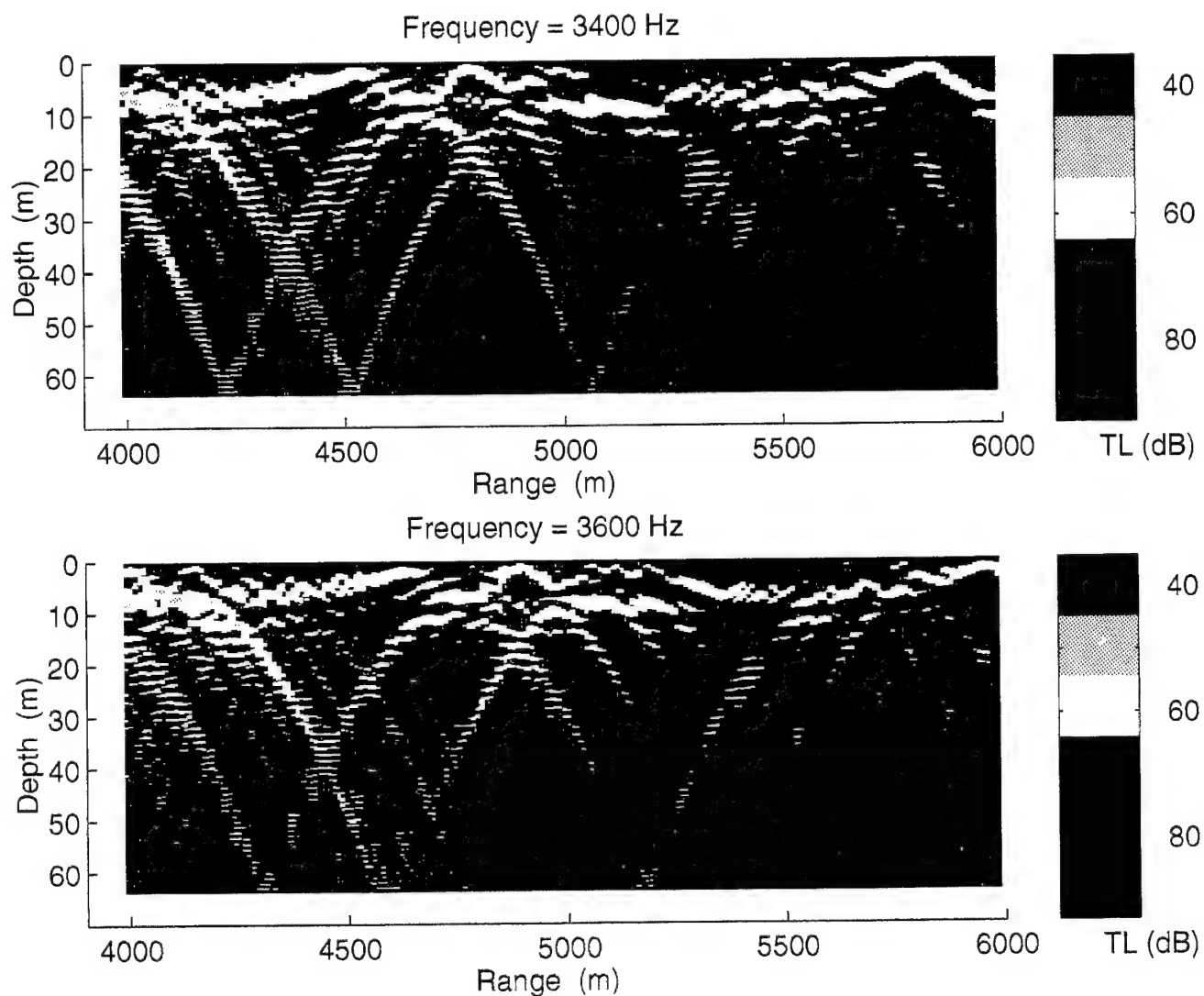is used.

Figure 11. Three dimensional TL plots by FEPE for 3.4 kHz
(upper) and 3.6 kHz (lower) (single frequency), for a
negative SSP overlying a silt/clay bottom; water depth is
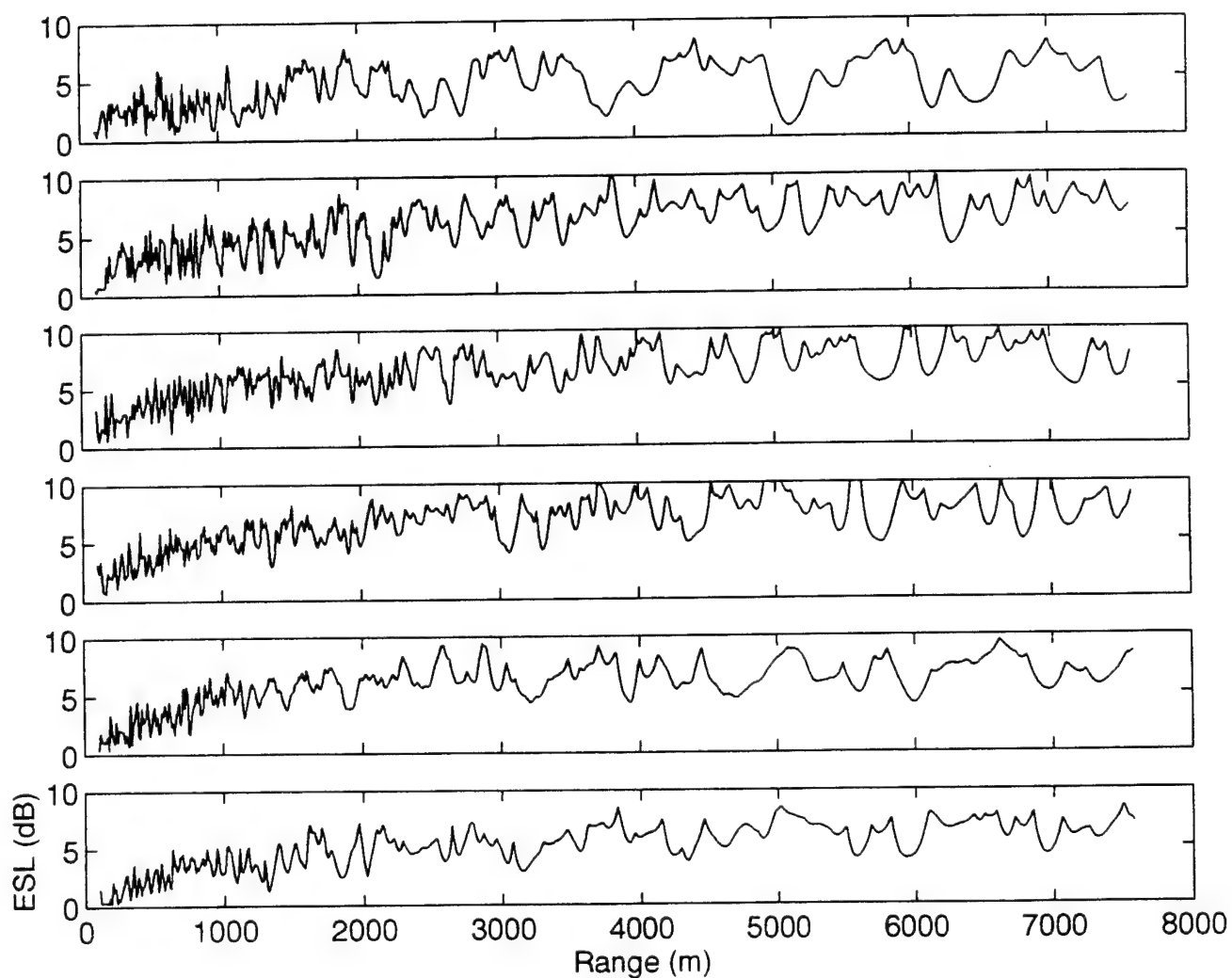64 m, source depth is 7.3 m.

Figure 12. ESL versus range plots for a negative SSP
overlying a sand bottom. Source depth is 7.3 m. Target
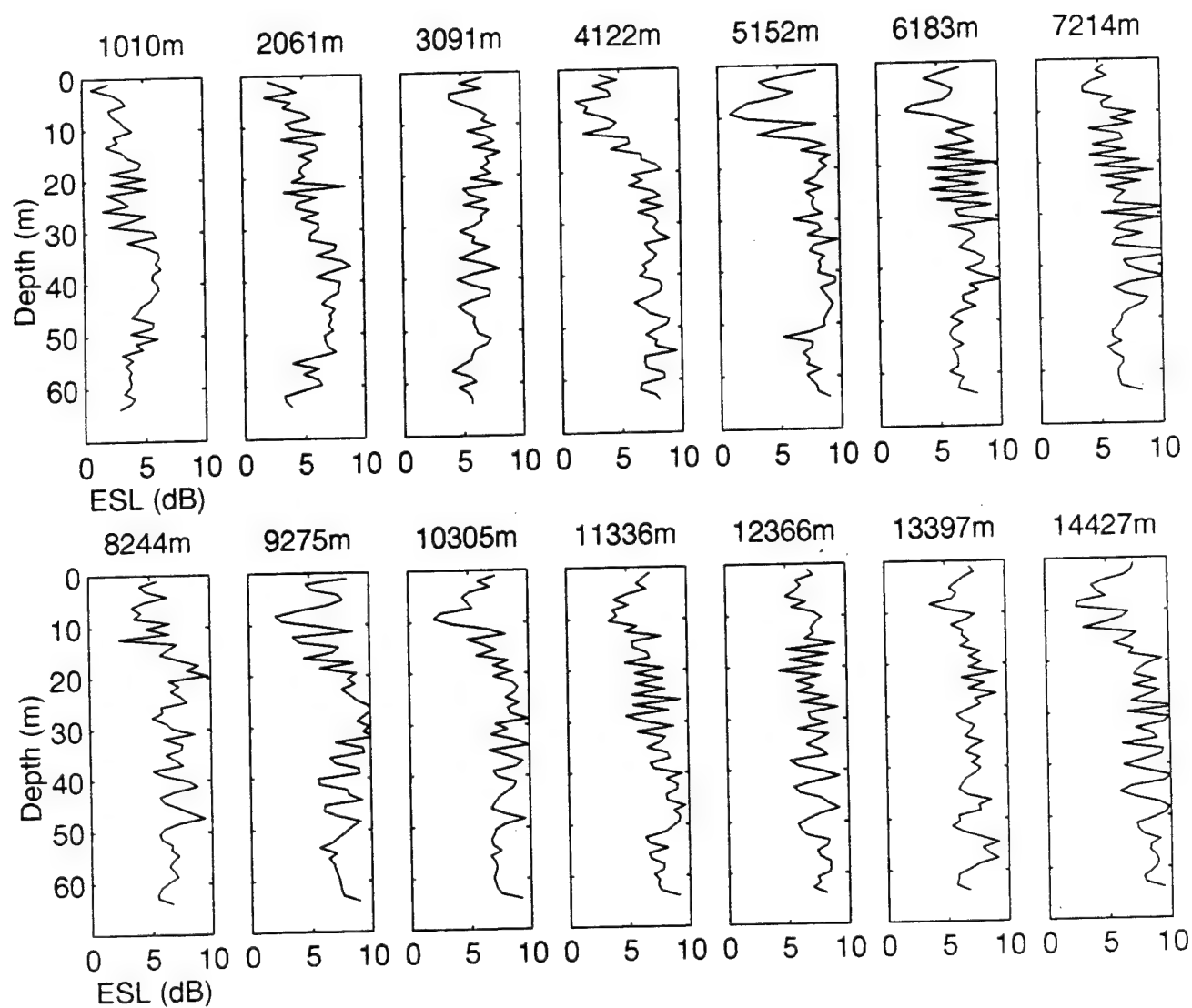depths are 10.3, 20.6, 30.9, 41.2, 51.5, 61.8 m,
respectively.

Figure 13. ESL versus depth plots for a negative SSP overlying a sand bottom. Source depth is 7.3 m. Ranges are shown on the top of each panel.
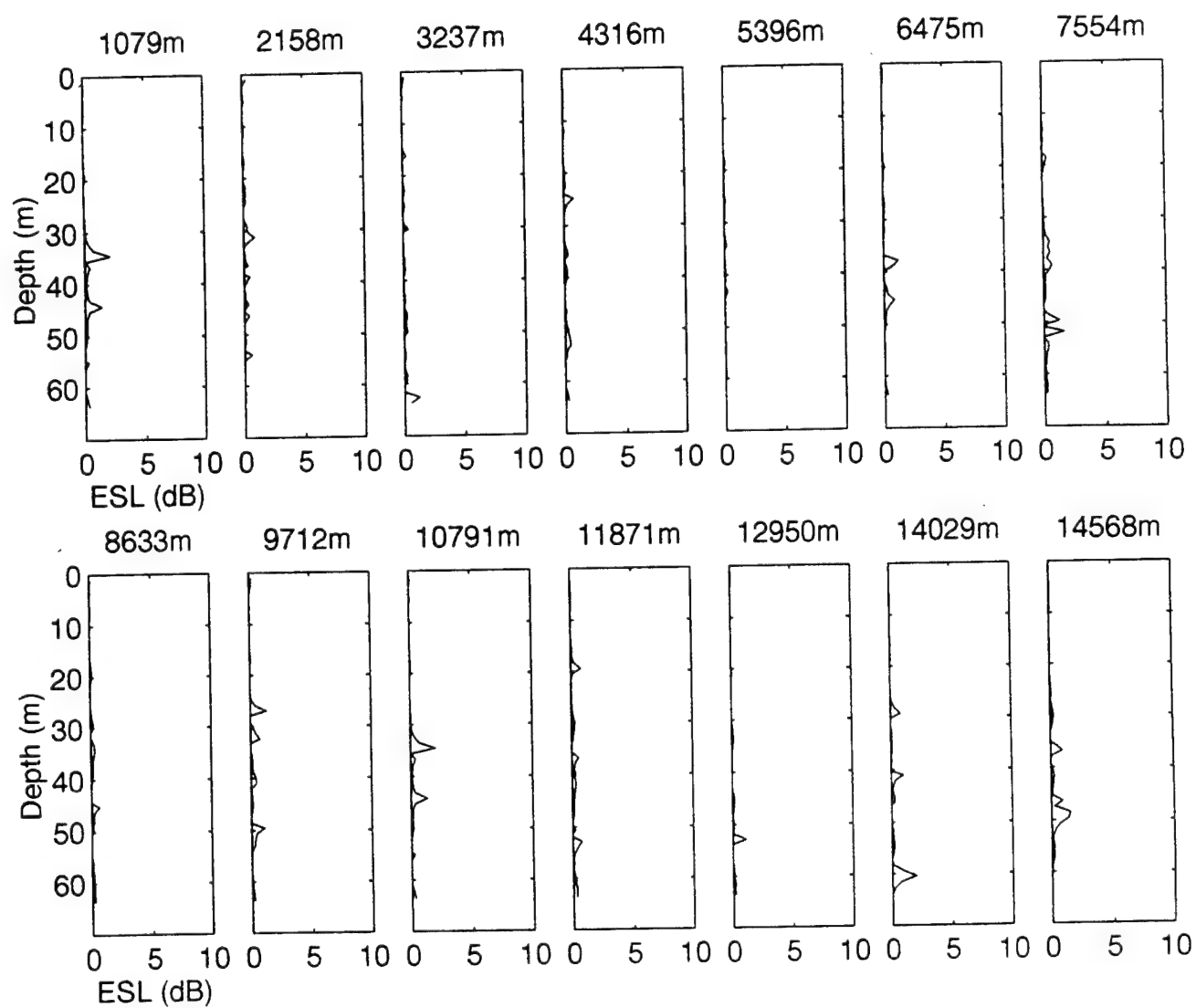
Figure 14. ESL versus depth plots for an isothermal SSP overlying a slow speed bottom. Source depth is 7.3 m. Ranges are shown on the top of each panel.
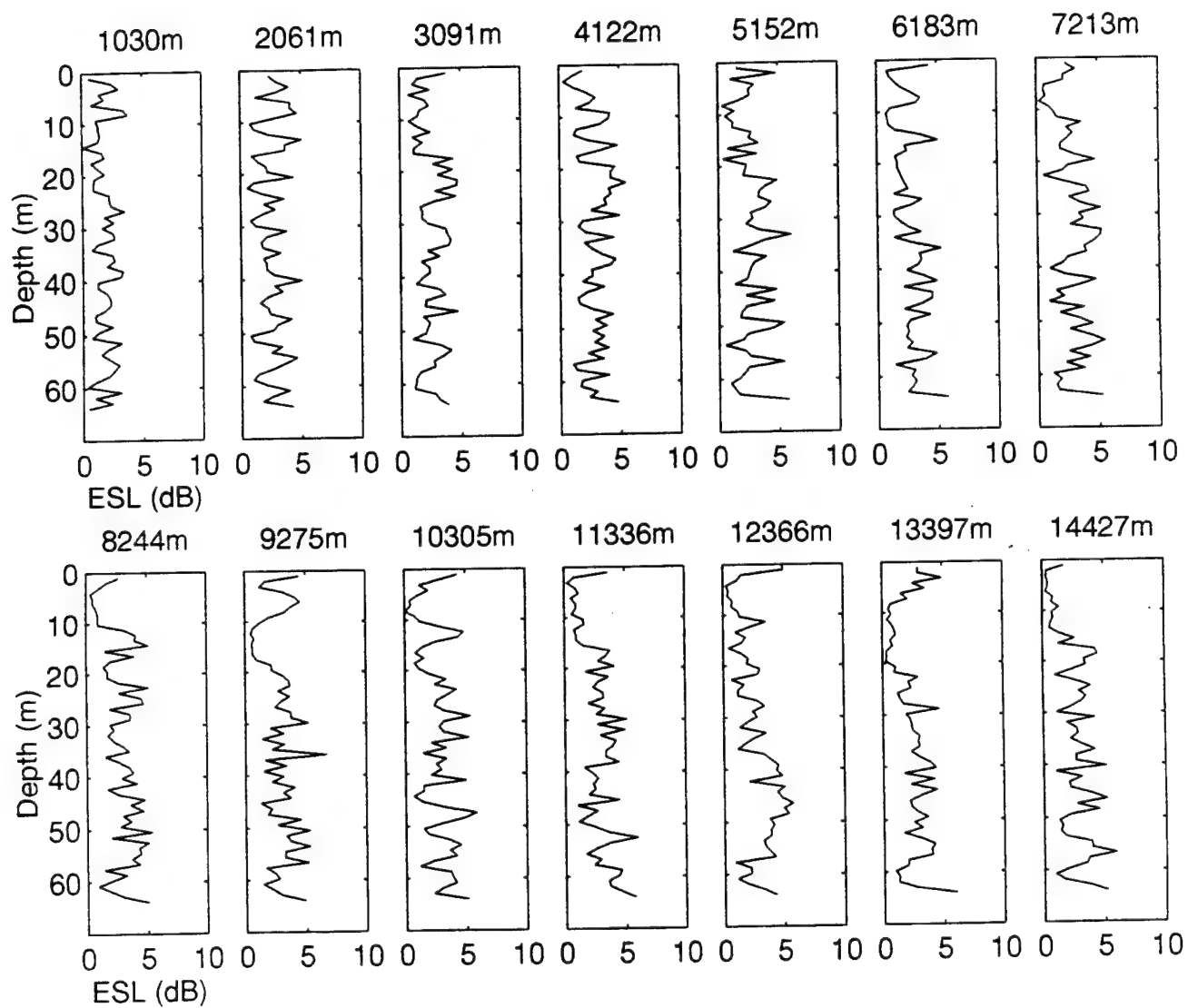
47

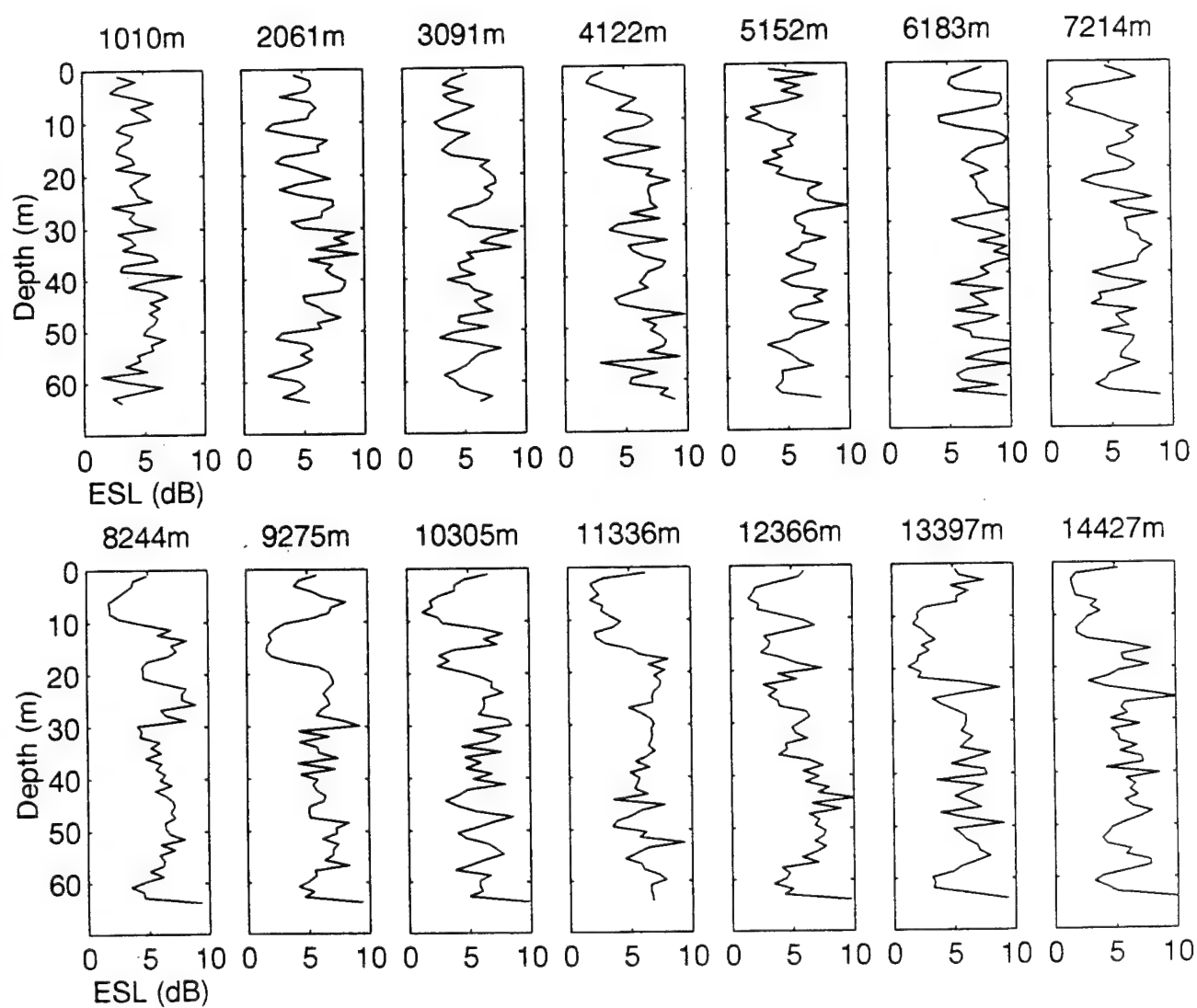Figure 15. Same as Figure 14 except for a silt/clay bottom.

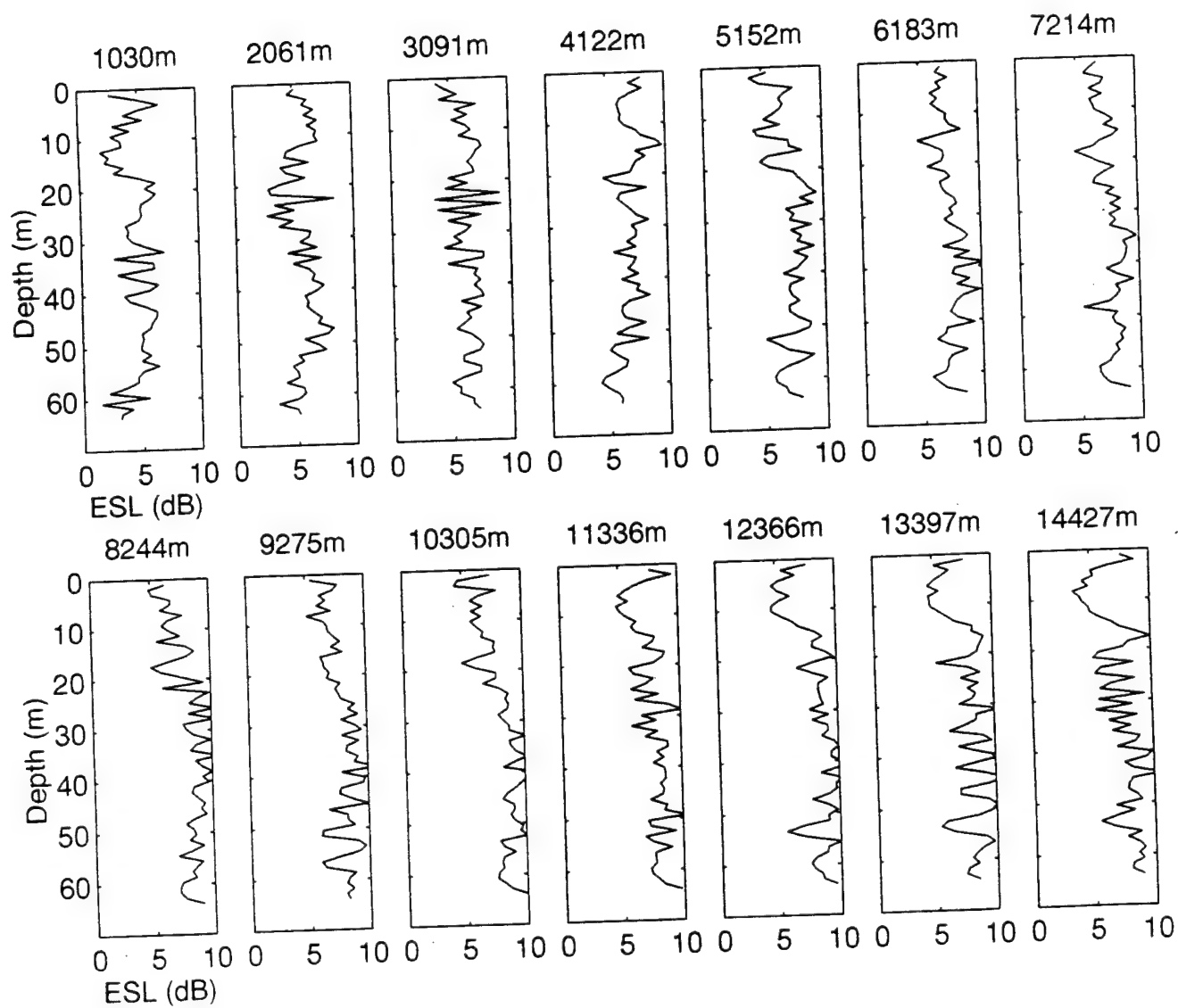48

Figure 16. Same as Figure 14 except for a sand bottom.

49

Figure 17. ESL versus depth plots for a ML-type SSP overlying a sand bottom. Source depth is 7.3 m. Ranges are shown on the top of each panel.

50

IV. OTHER ESL MEASURES

As discussed previously, several techniques have been introduced by various researchers to measure the amount of time stretching caused by multipath propagation. All suffer some degree of degradation due to assumptions inherent with each technique. In this chapter a quantitative comparison of three commonly used techniques is made with the ESL technique developed in this study.

A. TIME SPREADING STANDARD DEVIATION

The standard deviation of the time spreading, σ, (Equation (1-2)) and the average arrival time (Equation (1-3)) were calculated by a MATLAB program developed by the author for all data processed. Figures 18 and 19 show the normalized (by the peak value) ESL and σ as a function of depth and range, respectively. These two very different parameters compare favorably in a qualitative sense. However, there are depths and ranges where the correlation between ESL and σ is not good, and may be due to the fact that the distribution of the pulse time spreading is definitely not Gaussian (see Figures 3 through 5). Hence, the standard deviation may not be as meaningful as it would be if the distribution of the energy within the pulse were Gaussian.

51

B.   JONES' DEFINITION OF ESL

ESL based upon the definition of Jones (1990) (Equation (1-4)) was also computed by a MATLAB program developed by the author. Jones' theoretical approach is similar to the definition of ESL given in this study for a situation of a signal uncontaminated by noise. Both Equations (1-4) and (2-8) will yield identical results if the size of the resolution cell (the temporal resolution of the target system) is selected accurately. Unfortunately, it is difficult to determine the optimum duration of the resolution cell without first modeling ESL accurately. Jones suggested (1990) using a resolution cell width equivalent to the reciprocal of the pulse bandwidth, for this study $1/200 = 0.005$ sec.

When the peak pulse amplitudes of the time stretched pulses from the two techniques are compared, it is found that the Jones technique overestimates the magnitude of ESL by 2.4 dB. In order to bring the Jones technique into agreement with that of this study, the 2.4 dB reduction in peak amplitude is equivalent to increasing the resolution cell size to 0.0084 sec. The 0.0084 sec resolution cell size is not a general solution but is appropriate for short duration active pulses near 3.5 kHz. Accurate modeling of the time-stretched pulse is required to overcome the potential error in ESL if the resolution cell size is determined by a best guess.

52

C. MML

A normalized cross correlation of Equation (1-6) was also calculated by a MATLAB program developed by the author. Because of the simple temporal pulse shape, the coherence values were very high near the peak of the propagated pulse (Table 5) with a maximum value of 0.9999 obtained for the isothermal SSP, silt/clay case. This result supports the validity of the assumption that the shape of the pulse with no spreading and no reverberation is symmetric to the transmitted pulse described in Section B of Chapter II. However, the received pulse shape is not perfectly symmetric to the transmitted one. It is a little thinner than expected because the normalized cross correlation never reaches unity in this research, and several ESL values of around -0.0029 dB were observed for the isothermal SSP, silt/clay case. In the real ocean environment the MML will be severely degraded by the presence of reverberation (and ambient noise), and the high MML values obtained here for the model/signal-only case (i.e., no noise contamination) are expected to be high. A correlation beamformer with an advanced signal processor, such as Inverse Beamforming (IBF), offers great promise in regaining/ overcoming sonar system performance degradation due to ESL in shallow water.

For the tactical active sonar, matched filter or correlation processing is the heart of the detection system. When the signal gives low coherence (equivalent to the

53

normalized cross correlation given by Equation (1-6)) below a previously selected threshold, it is recognized as a false signal. Jensen and Sabbadini (1993) demonstrated the impact of the signal coherence by defining the MML for a LFM signal with bottom interaction in deep water. One expects this may have significance when sophisticated pulses such as LFM signals are used in shallow water. Coherenced-based signal processing/ beamforming methods used with peak pickers for post processors show great promise in regaining ESL due to time stretching.[Nuttall and Wilson, 1991; Wilson, 1995; Fabre and Wilson, 1995]

Table 5. The coherence (normalized cross correlation) for an isothermal SSP overlying a silt/clay bottom

| Range(m)	Mean coherence	std coherence	Max coherence	Min coherence
1030	.9265	.053	.9912	.7914
2061	.9337	.050	.9956	.8233
3091	.9312	.064	.9951	.7237
4122	.9222	.057	.9898	.7601
5152	.9338	.060	.9949	.7205
6183	.9121	.074	.9983	.6897
7213	.9297	.061	.9978	.7055
8244	.9327	.048	.9950	.8163
9275	.9298	.051	.9932	.7307
10305	.9348	.053	.9970	.7566
11336	.9346	.063	.9950	.7299
12366	.9417	.067	.9976	.5524
13397	.9607	.035	.9965	.8307
14427	.9524	.048	.9982	.7715
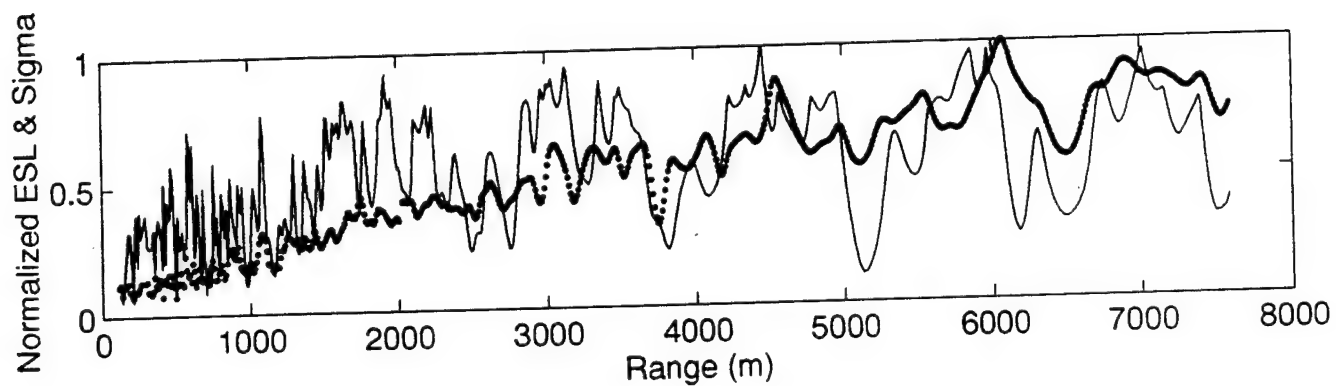
Figure 18. Comparison of ESL to time spreading standard
deviation for a negative SSP overlying a sand bottom.
Source depth is 7.3 m, target depth is 10.3 m. The solid
line represents ESL, the dots represent the standard
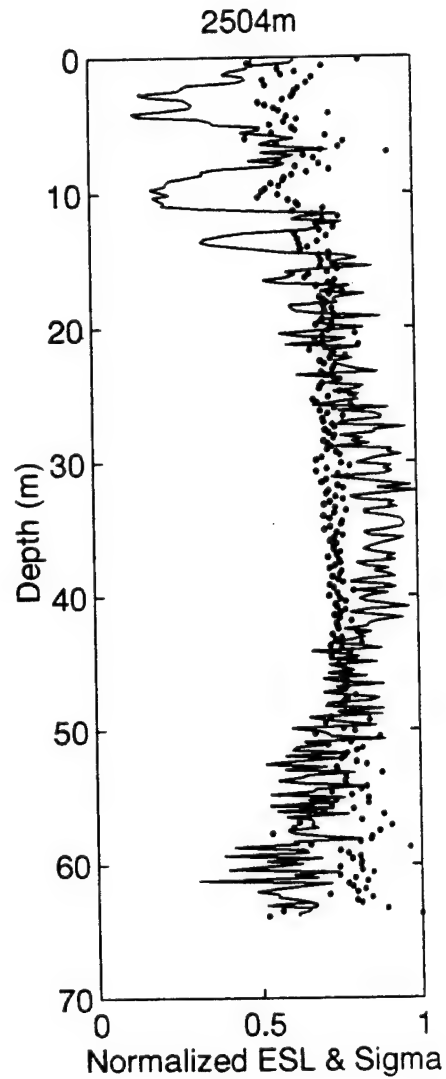deviation.

56

Figure 19. Comparison of ESL to time spreading standard
deviation for a negative SSP overlying a sand bottom.
Source depth is 7.3 m, range is 2504 m. The solid line
represents ESL, the dots represent the standard deviation.

57

V. IMPACT OF ESL ON TACTICAL ACTIVE SONAR PERFORMANCE IN SHALLOW WATER

A. IMPACT OF ESL ON TOTAL LOSS

According to the ESL analysis in the previous chapter, it is the bottom boundary geoacoustic properties that dominate the behavior of both TL and ESL. Thus, a tactically important SSP is one exhibiting a negative profile because this SSP refracts acoustic energy downward towards the bottom boundary. It was the negative SSP overlying sand (reflective) bottom which exhibited the highest ESL. In contrast, when this SSP overlies a silt/clay (absorptive) bottom, the ESL is significantly reduced (4 dB or more), but as expected, the TL is also very large.

Figure 20 shows an example of the received pulses for the negative SSP overlying a silt/clay bottom. Compared to the stretching observed in Figures 3 through 5, one sees for this case that the time stretching is minimal; the pulses associated with the higher modes which lead to the time dispersion are absorbed by the bottom. This is borne out in the ESL vs range plots where the sand (reflective) bottom (Figure 21), shows ESL to be ~ 3 to 4 dB higher than for the silt/clay (absorptive) bottom (Figure 22).

In spite of the low ESL for a silt/clay bottom, the overall detection range is degraded because TL is extremely large. Thus, a reflective sand bottom probably offers the best

59

detection opportunity because of the reduced TL. If signal processing methods can be developed to regain the loss due to energy spreading, then sandy, reflective bottoms can be anticipated to offer even greater detection opportunities.

The impact of the bottom sediment on sonar performance is further illustrated by comparing the total transmission loss (ESL + TL) and TL only for propagation over sandy and silty bottoms (Figures 23 and 24). The difference between the curves on each plot is the ESL. Note that as stated previously, the two curves are almost coincident for the silt/clay bottom (i.e., ESL is small) but widely separated for the sand bottom (ESL large). However, better sonar performance is not realized in areas covered by silt/clay (absorptive) sediments because the potential gain achieved by low ESL is offset by a much larger TL.

B. ANALYSIS OF ESL IN DEEP WATER

Although ESL is significant in shallow water environments due to multipath effects, ESL isn't as large in deep water because a single, or nearly similar multipaths, dominates the time arrival structure. For passive sonars at very long ranges one can measure significant time dispersion even in deep water, but tactical active sonar detection ranges are usually very short. Ray theory is usually a good approximation and the time stretching is usually minimal in deep water. Figure 25 shows the TL for a single frequency 3500 Hz signal in shallow

60

water where a deep sound channel (SC) sound speed profile with axis at 25 m has been simulated to illustrate this ESL deep water dependence.

Although this is not a realistic situation, Figure 25 shows the impact of the SC-type SSP on TL. ESL vs depth plots for the received pulses are shown in Figure 26. Comparing the impact of ESL to the negative SSP case (Figure 13), ESL is far less significant for the deep water, SC propagation. Figure 27 shows TL + ESL vs depth plots for this case. It is evident that at depths where TL is small, ESL is also small. Therefore ESL is not significant in the deep water, short range SC propagation environment.

C.   ANALYSIS OF DEEPER SOURCE DEPTH

So far the analysis has been performed only for the source depth (SD) of 7.3 m, chosen to represent the typical depth for a bow mounted sonar. However, we must consider variable depth, tactical sonars which can be deployed from an ASW helicopter. Although this sonar can change its operational depth, the optimum depth for performance can be found by computing a number of FEPE runs at various source depths for a single frequency (3500 Hz). We selected a source depth of 51.5 m as optimum based on analysis. Figures 28 and 29 depict the TL for a negative SSP overlying a sand and silt/clay bottom, respectively. Figure 30 and 31 show the ESL vs depth plots for the above two cases. Comparing Figure 13 (shallow

61

source) to Figure 30 for the sand bottom, ESL is seen to decrease as the source depth increases. Examining both received pulses in the time domain, the observed number of time spread pulses significantly decreased from the order of 20 for the shallow source to the order of 5 for the deep source. This indicates that bottom interaction was decreased for a near bottom source, resulting in fewer pulses and less time spreading. The same result is obtained for the silt/clay bottom as seen in the comparison of Figures 22 and 31. In this case, even fewer pulses were observed for the deep source depth.

In Figures 28 and 29, the direct path energy from a deep source propagates to great ranges (up to 8000 m range). Accordingly, for the negative SSP with the deeper source depth, propagating energy for depths near the bottom is not attenuated as readily as for the shallow source. Propagating modes exist in the deeper depth region and, combined with the reduced ESL impact for the deeper source, implies that improved performance may be anticipated for the variable depth sonar when lowered to depths well below the surface.

D. COMPARISON OF BROADBAND PULSE TO SINGLE FREQUENCY PROPAGATION

Although FEPE is being adopted as the new Oceanographic and Atmospheric Master Library (OAML) standard acoustic propagation model by the U.S. NAVY, FEPE predicts the TL only

for a single frequency, which contains no temporal spreading information. In reality, pulses with finite bandwidths are used in all tactical active sonars. To illustrate the difference between a single and multiple-frequency TL, TL plots for both a single frequency (3.5 kHz) and a 200 Hz band pulse centered at 3.5 kHz are shown in Figure 32 for a 10.31 m target depth for the negative SSP, sand bottom case. The thin line shows the single frequency (3.5 kHz) FEPE TL estimate, and the thick line shows the FEPE_SYN TL estimate for the broadband pulse. The 200 Hz pulse shows less TL fluctuations with range than the single frequency TL. This is the result of convolution (or Fourier synthesizing) of 200 frequency bins of energy which behaves like incoherent summation. This is tactically important because for the shallow water wave guide, TL will not fluctuate severely, but will increase rather smoothly as will the probability of detection curve. To illustrate this effect on ESL Figure 33 shows the total loss (200 Hz band) and single frequency TL (3.5 kHz) vs range for the same inpit parameters. ESL degrades the total loss by 1 to 8 dB. This means that a single frequency FEPE TL estimate can underestimate the total loss from 1 to 15 dB in shallow water.

Consequently, for tactical active sonars, the performance should be predicted using the transmitted pulse TL, not the single frequency TL.

63

E. EFFECT ON SMALL SCALE CHANGES IN TARGET DISPLACEMENT

The total loss vs range or depth plots (e.g., lower panels of Figure 23 and 27) indicate that small range and depth scale changes can possibly be significant. Because of computational efficiency, the resolutions of all the previous plots were selected with a range increment of 10.31 m and a depth increment of 1.03 m. Figure 34 shows ESL calculated for range increments, 10.31 m and 0.412 m for the negative SSP, sand bottom case. This figure shows that the coarse horizontal resolution replicates the features of the transmitted pulse satisfactorily. Similarly, a coarse (1.031 m) and a fine (0.206 m) depth increment intercompared. Figure 35 shows that the coarse vertical increment replicates the transmitted pulse satisfactorily but exhibits finer-scale fluctuations that are not reproduced by the coarse depth resolution.

These figures also demonstrate that the total loss is not as sensitive to horizontal array displacements as for vertical displacements. Thus, the sonar array should be vertically stabilized physically or electronically.
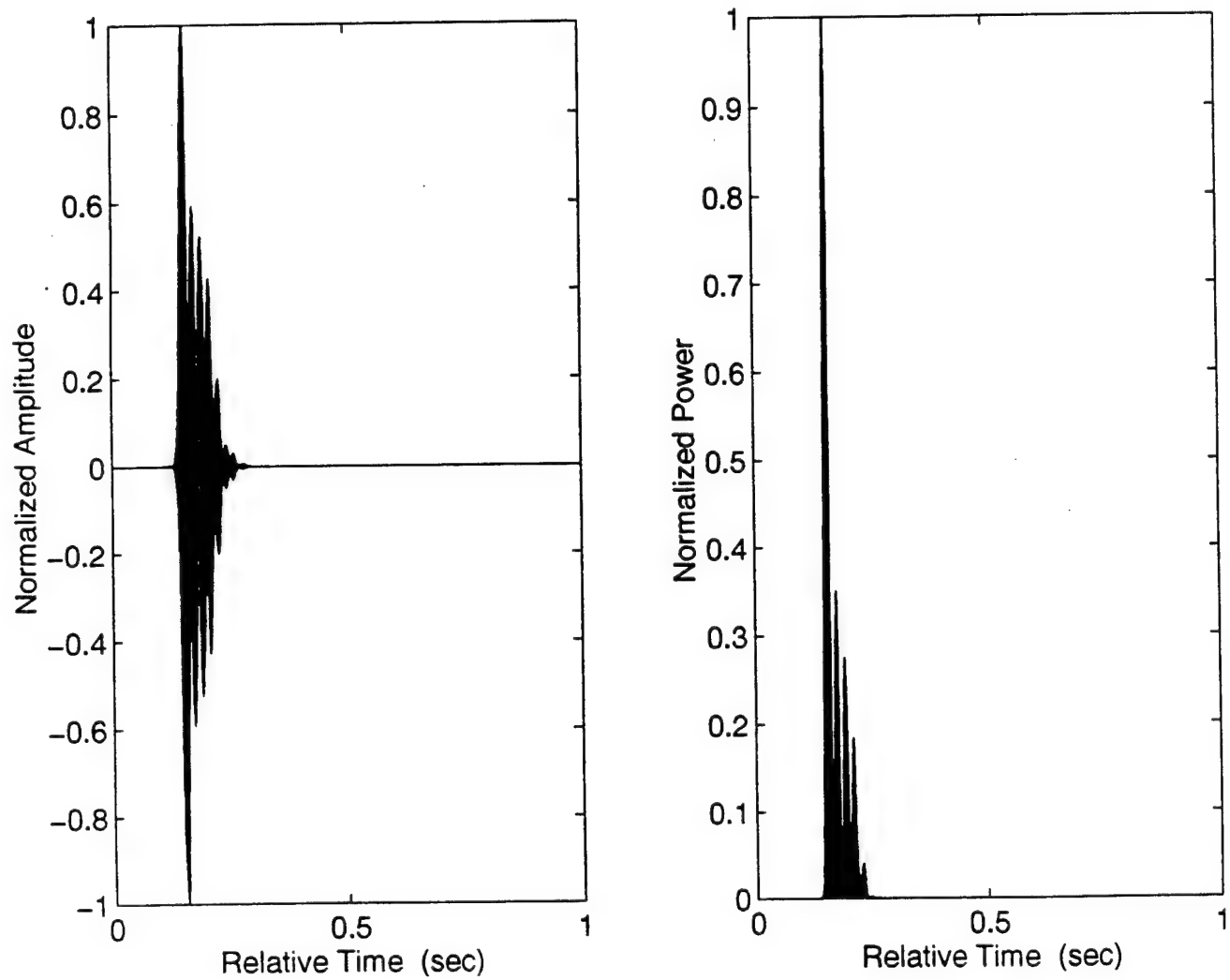
Figure 20. An example of the received pulse shape for a negative SSP overlying a silt/clay bottom, source depth is 7.3 m. ESL is 2.0 dB.
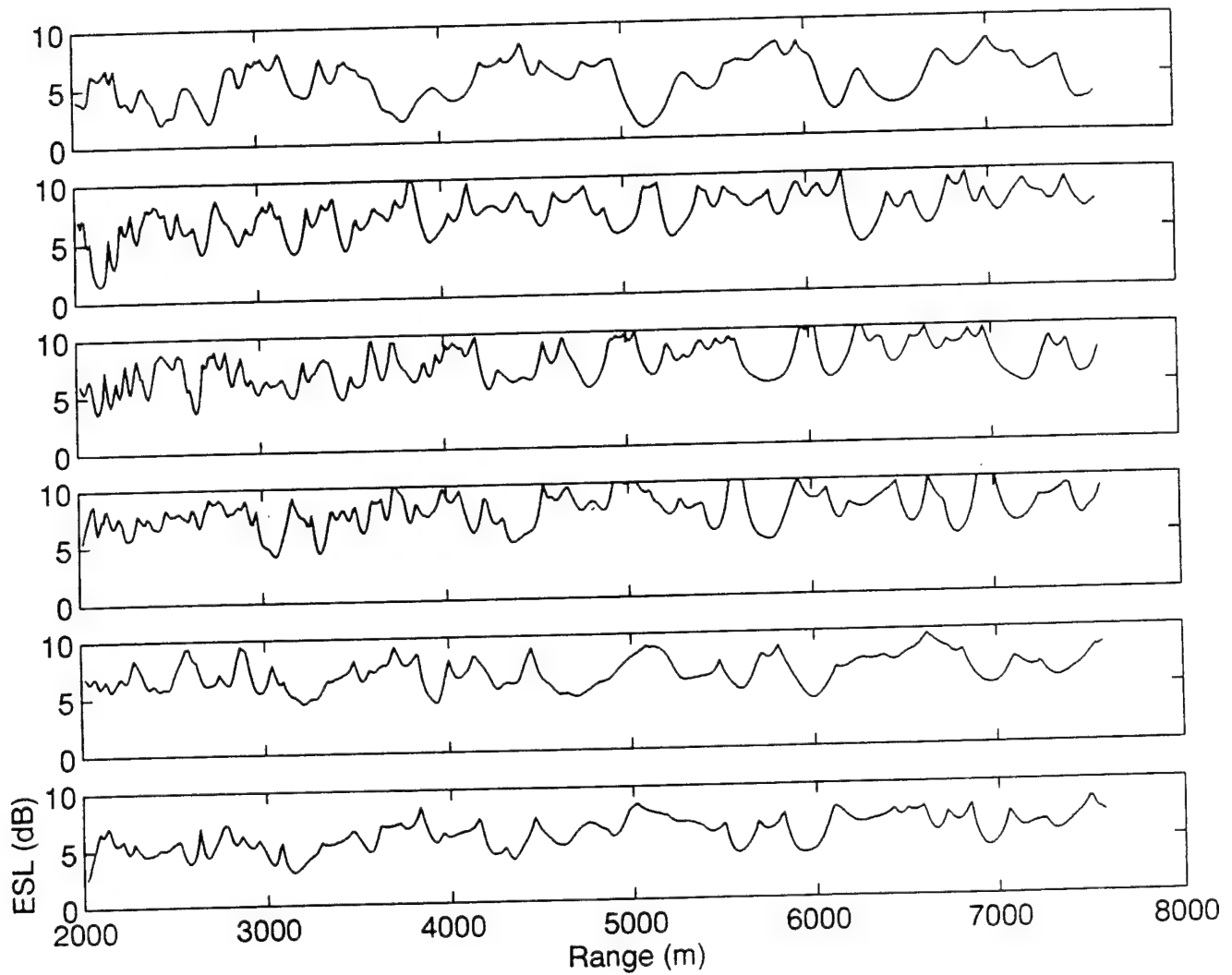
Figure 21. ESL versus range plots for a negative SSP overlying a sand (reflective) bottom. Source depth is 7.3 m. Target depths are 10.3, 20.6, 30.9, 41.2, 51.5, 61.8 m, respectively.
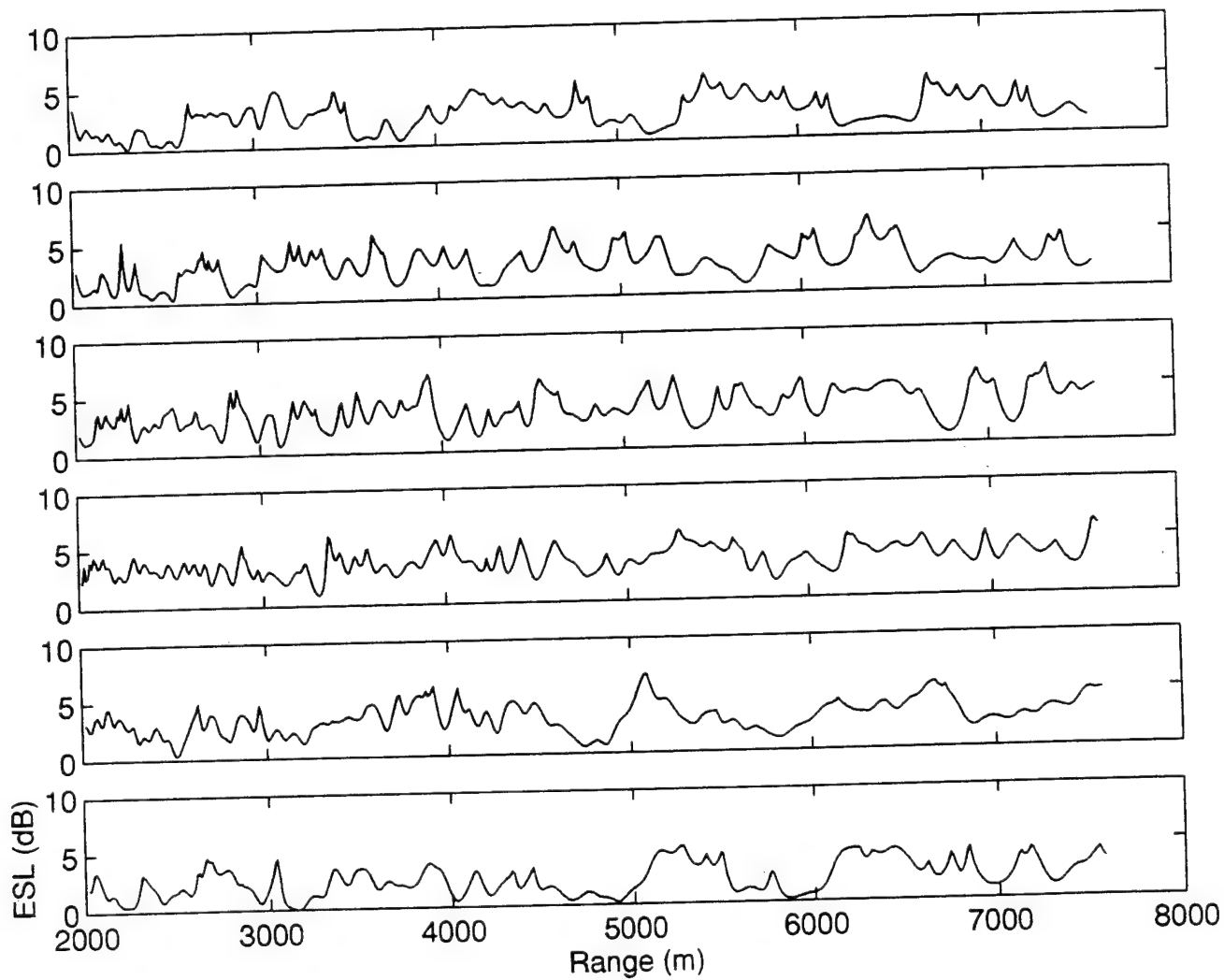
Figure 22. Same as Figure 21 except for a silt/clay (absorptive) bottom.
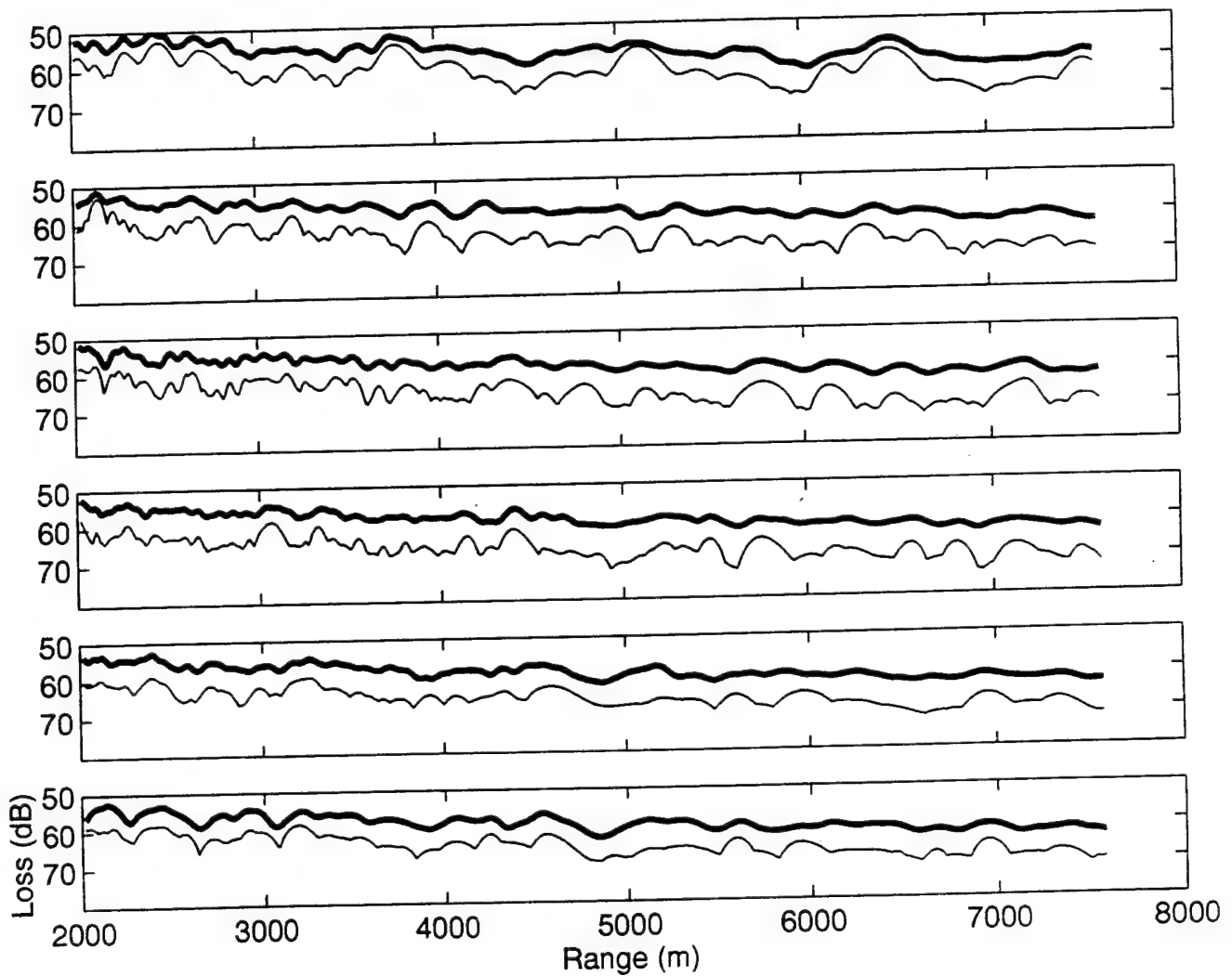
67

Figure 23. Total loss and TL versus range plots for a negative SSP overlying a sand (reflective) bottom. Source depth is 7.3 m. Target depths are 10.3, 20.6, 30.9, 41.2, 51.5, 61.8 m, respectively. The thick line represents TL, the thin line represents total loss (TL + ESL).
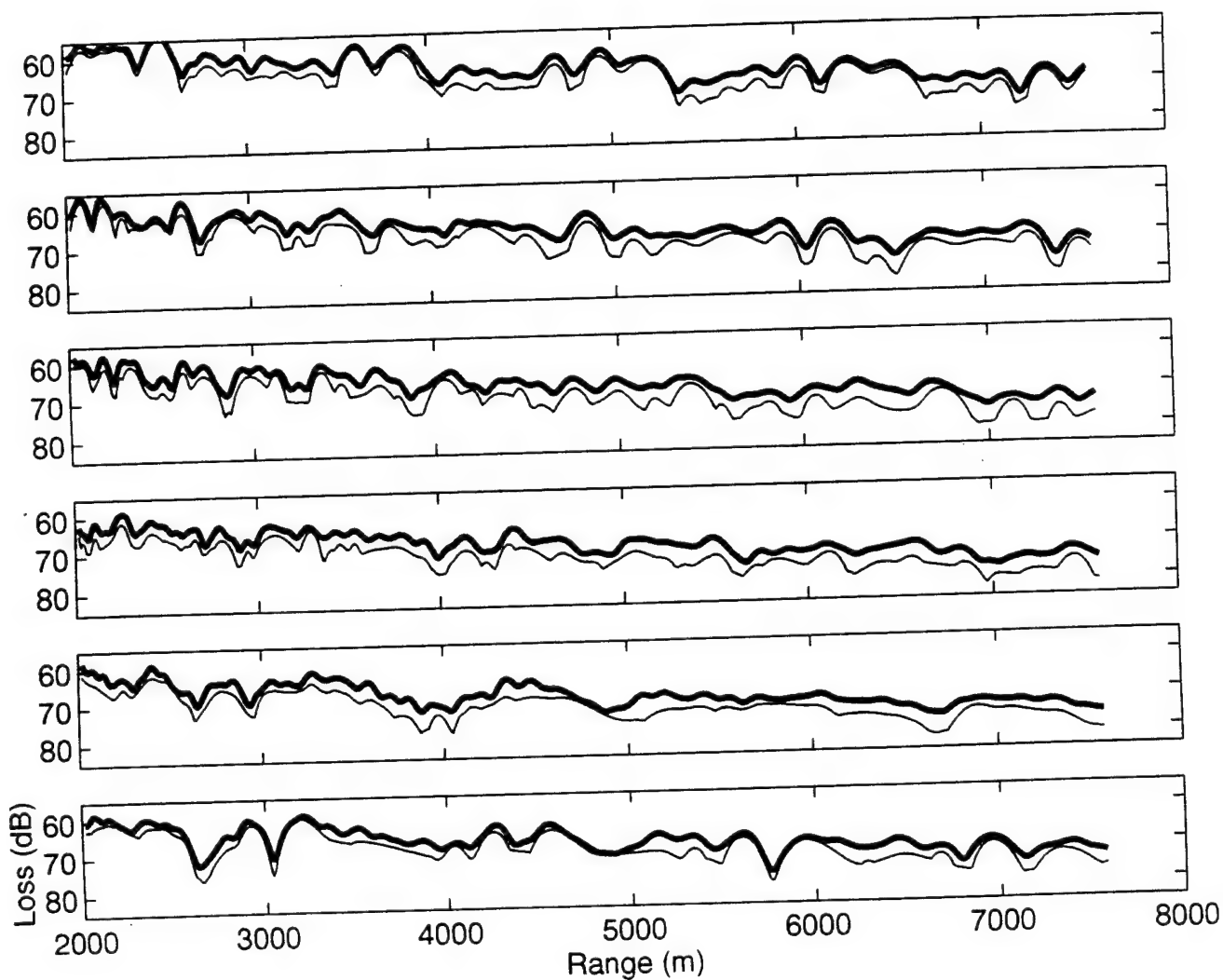
Figure 24. Total loss, TL versus range plots for a negative
SSP overlying silt/clay (absorptive) bottom. Source depth
is 7.3 m. Target depths are 10.3, 20.6, 30.9, 41.2, 51.5,
61.8 m from the top panel, respectively. The thick line
represents TL, the thin line represents total loss (TL +
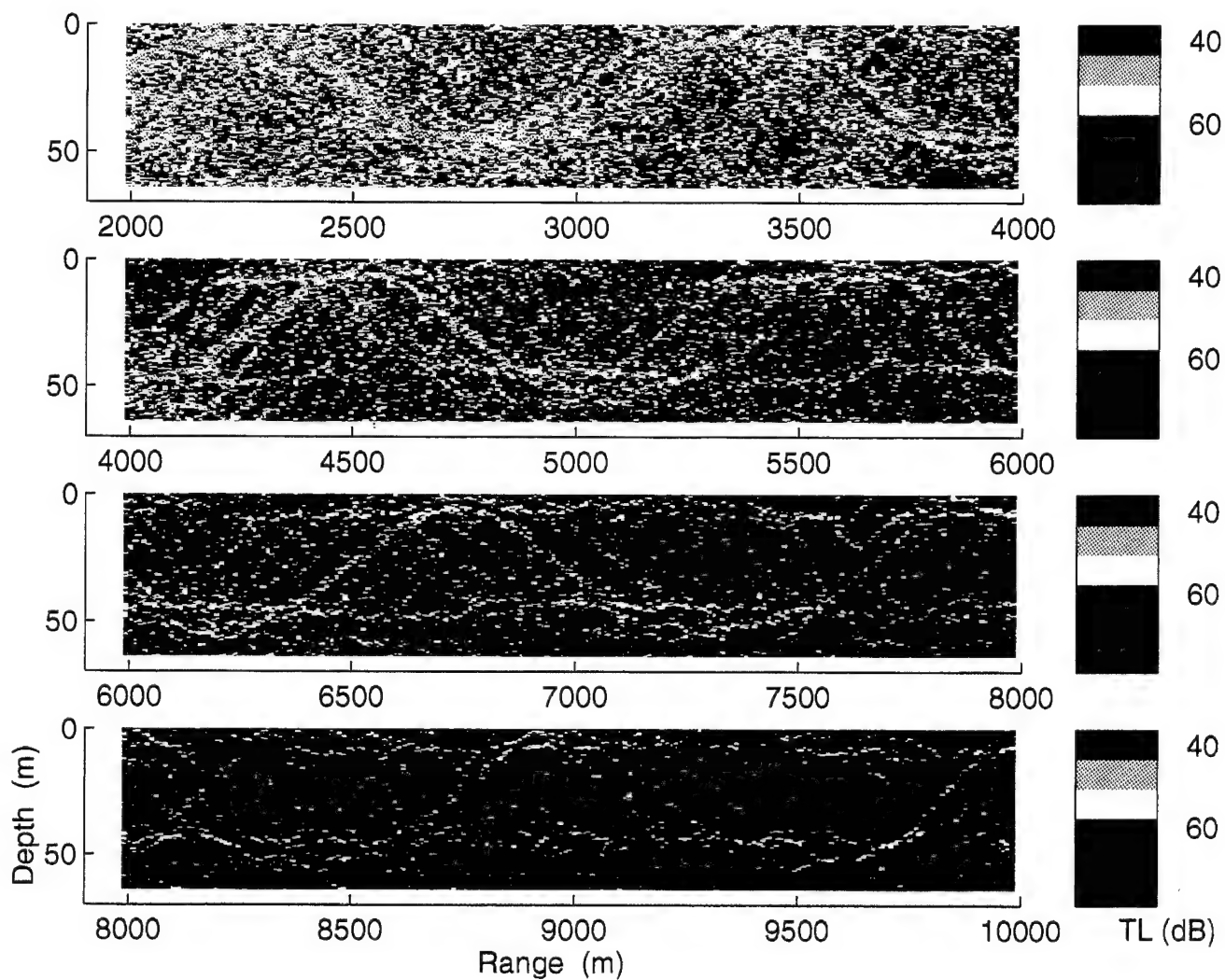ESL).

69

Figure 25. Three dimensional TL plots by FEPE for 3.5 kHz
(single frequency) for a SC-type SSP overlying a sand
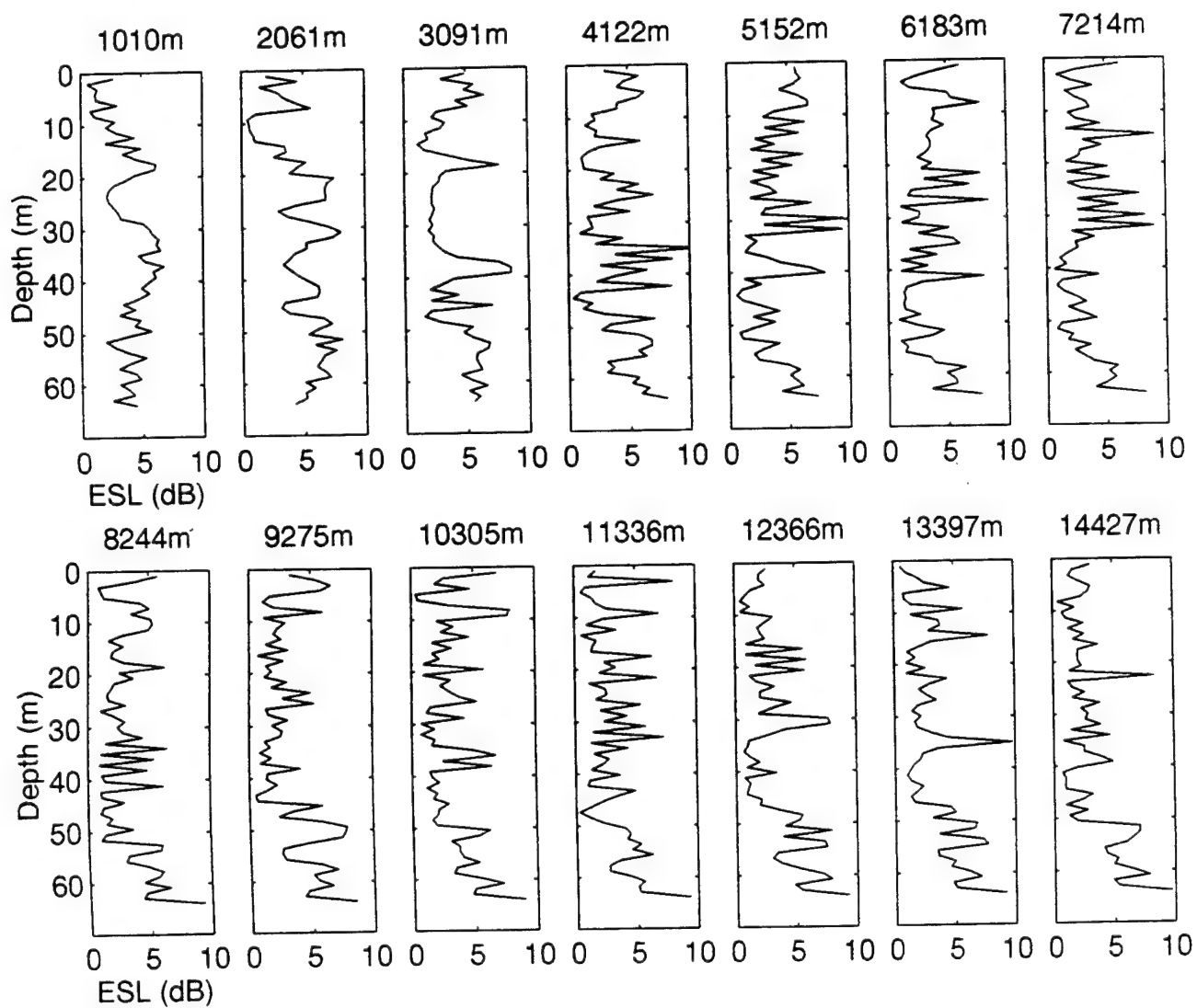bottom; water depth is 64 m, source depth is 7.3 m.

70

Figure 26. ESL versus depth plots for a SC-type SSP overlying a sand bottom. Source depth is 7.3 m. Ranges are shown on the top of each panel.
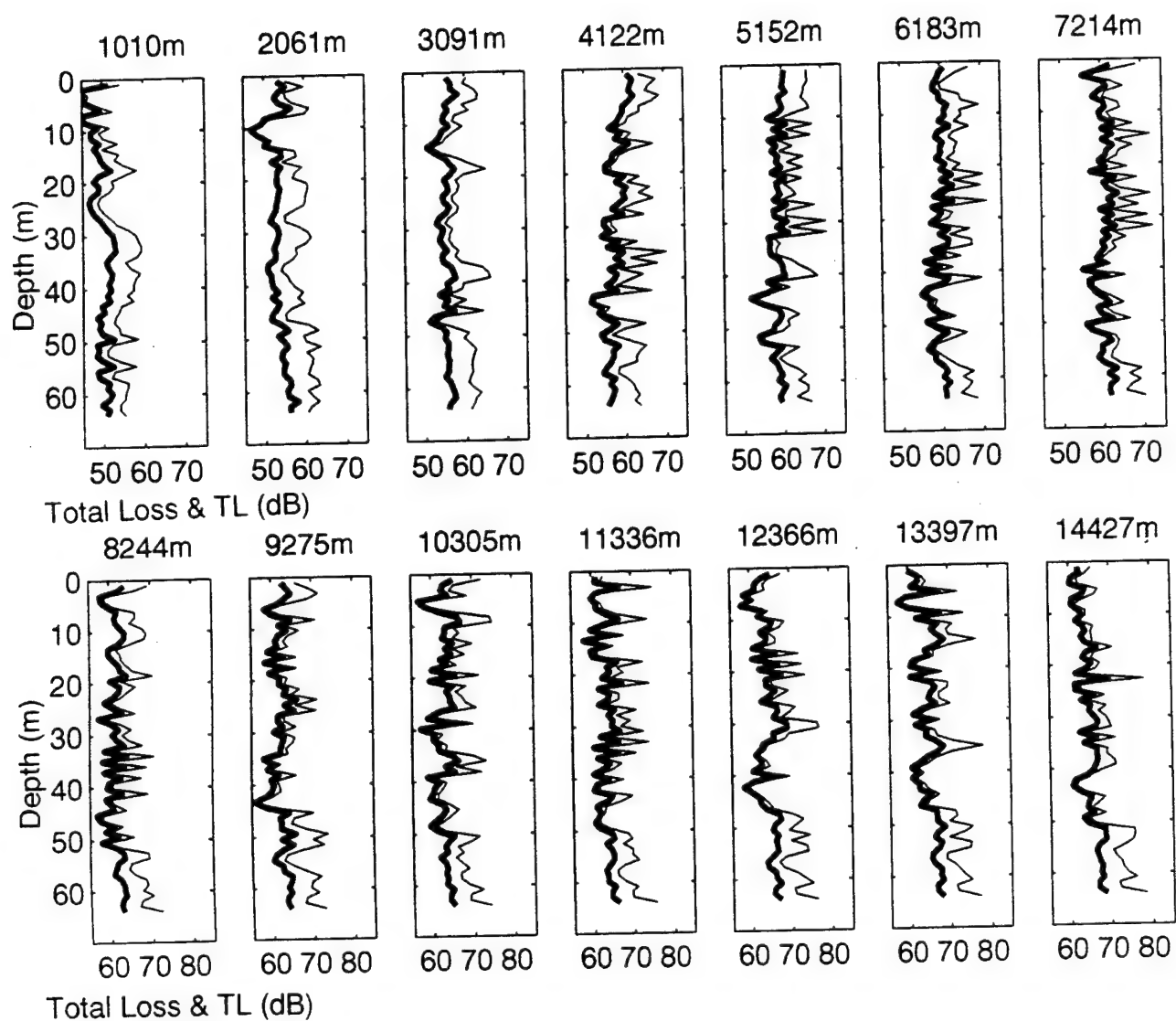
Figure 27. Total loss and TL versus depth plots for a SC-type SSP overlying a sand bottom. Source depth is 7.3 m. Ranges are shown on the top of each panel.

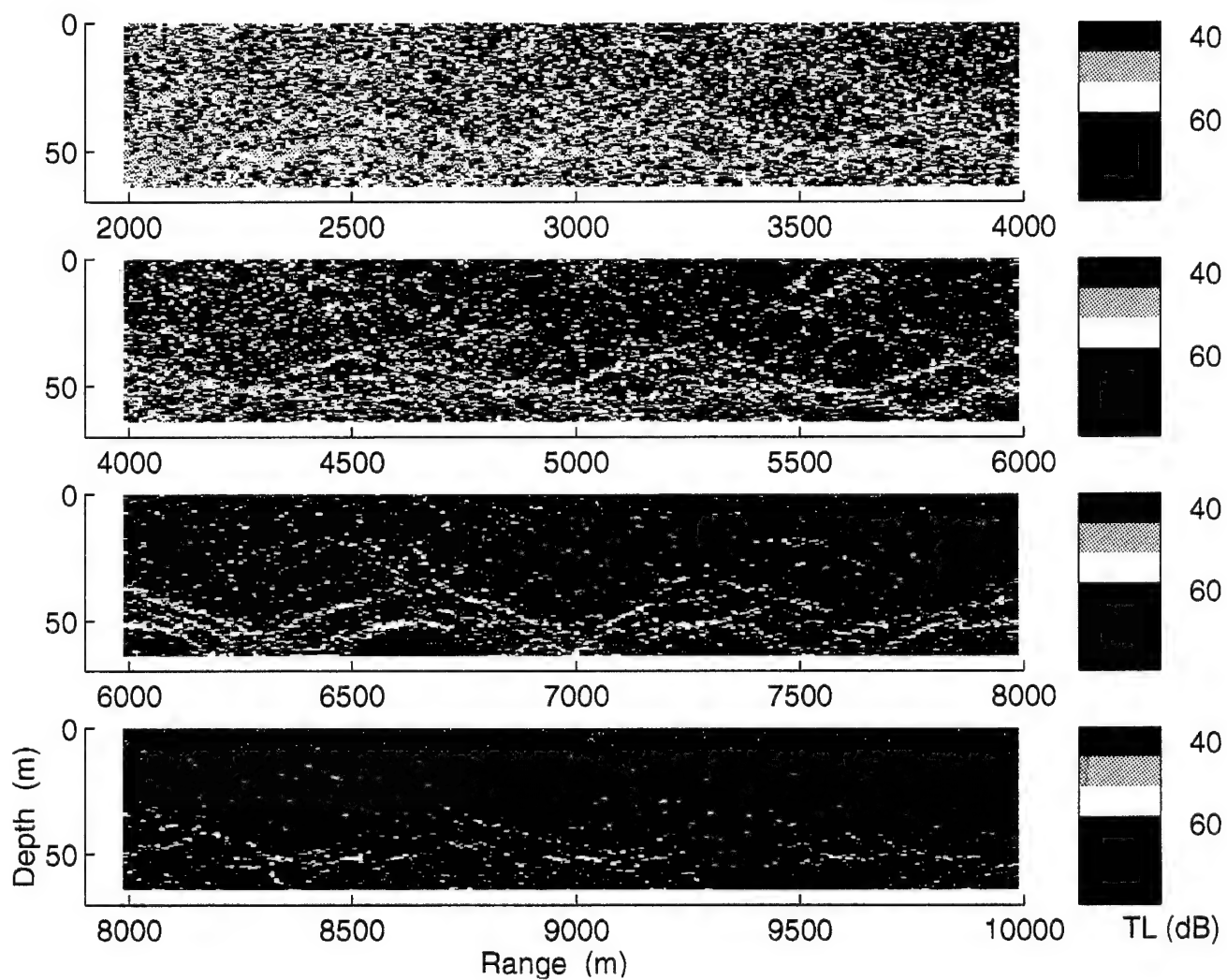Figure 28. Three dimensional TL plots by FEPE for 3.5 kHz
(single frequency) for a negative SSP overlying a sand
bottom; water depth is 64 m, source depth is 51.5 m.

73
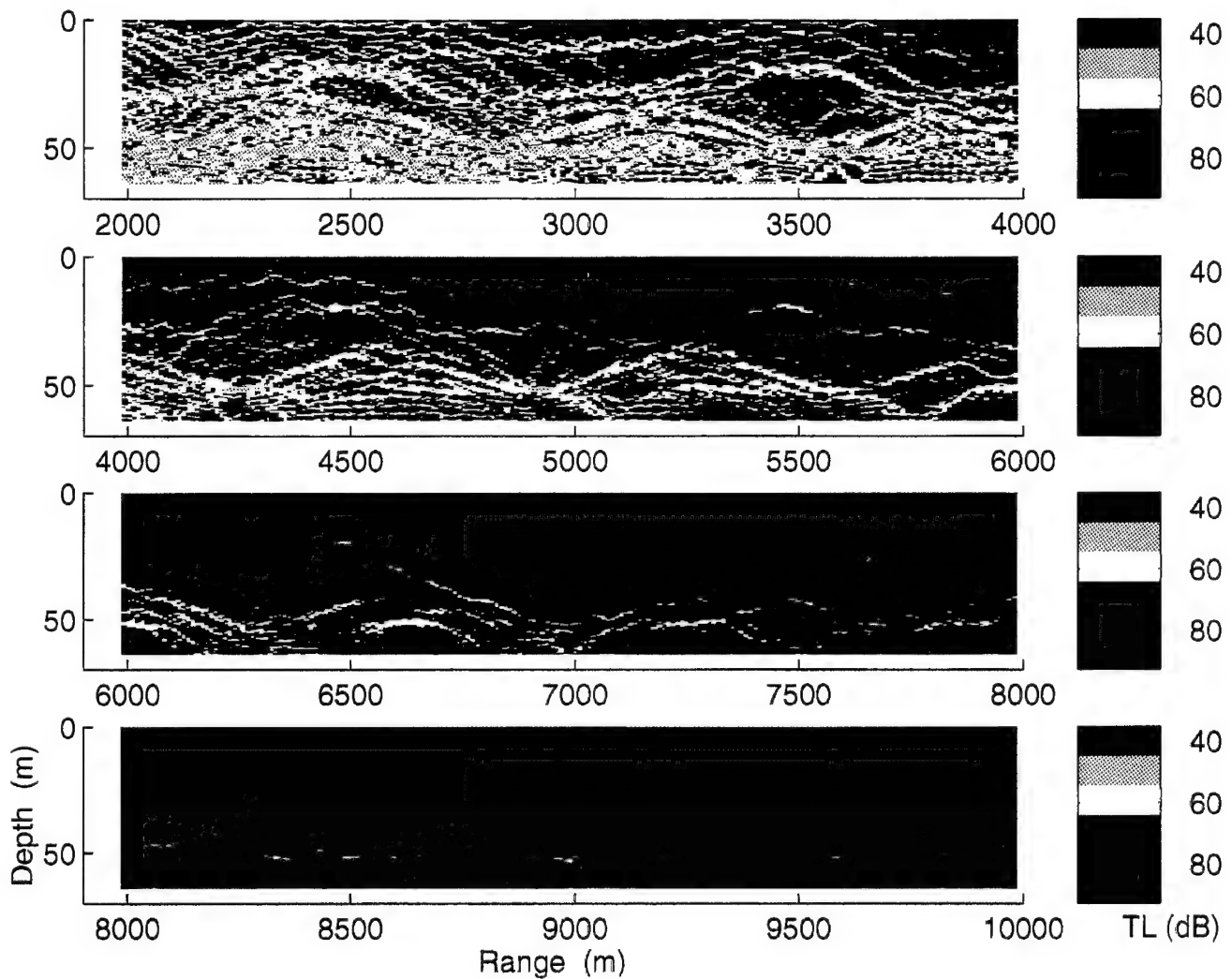
Figure 29. Three dimensional TL plots by FEPE for 3.5 kHz
(single frequency), for a negative SSP overlying silt/clay
bottom, water depth is 64 m, source depth is 51.5 m. The
color bar scale was changed due to large TL for this case.
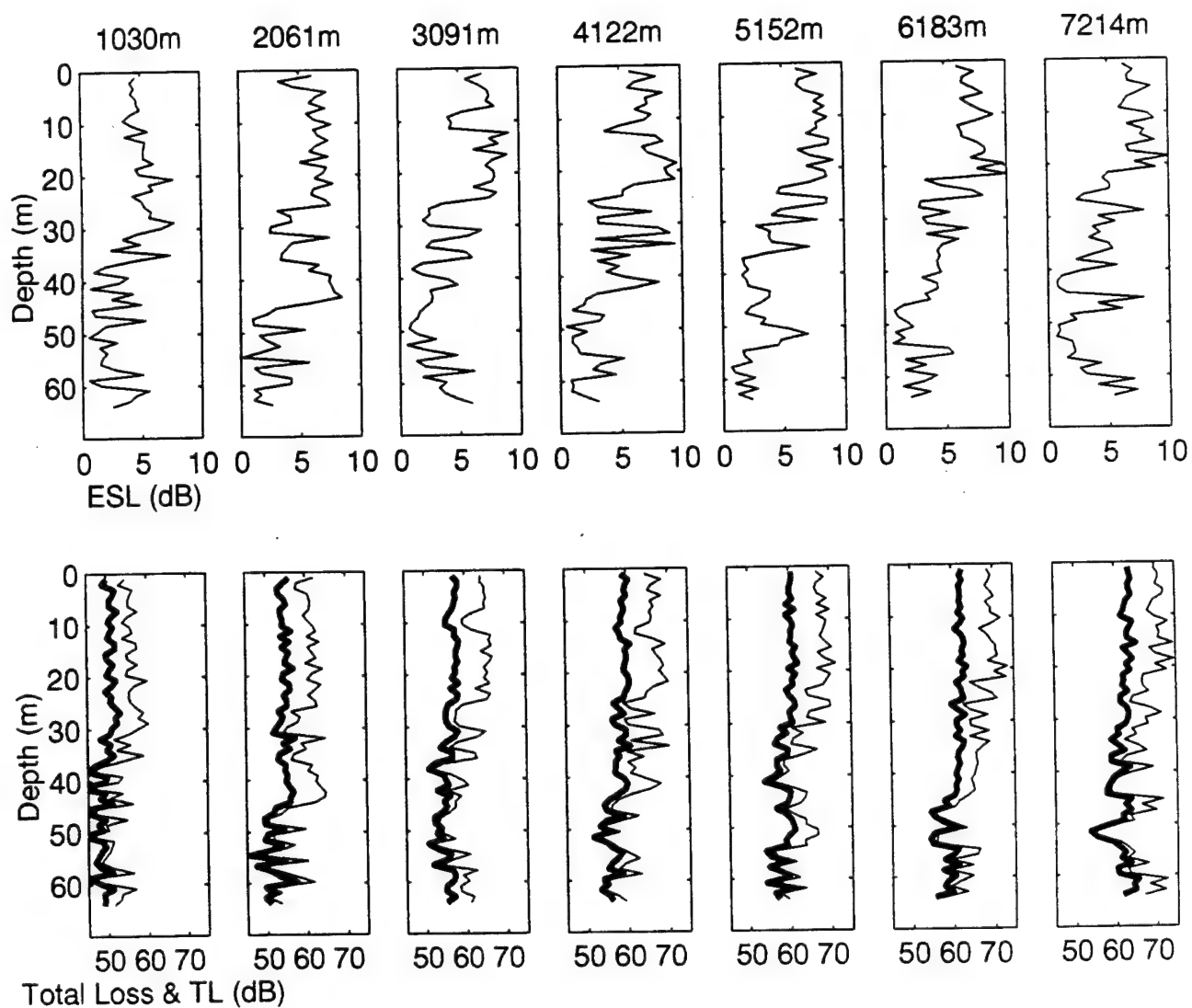
Figure 30. ESL versus depth plots (upper panels) and total loss and TL versus depth plots (lower panels) for a negative SSP overlying a sand bottom. Source depth is 51.5 m. Ranges are shown on the top of each panel.
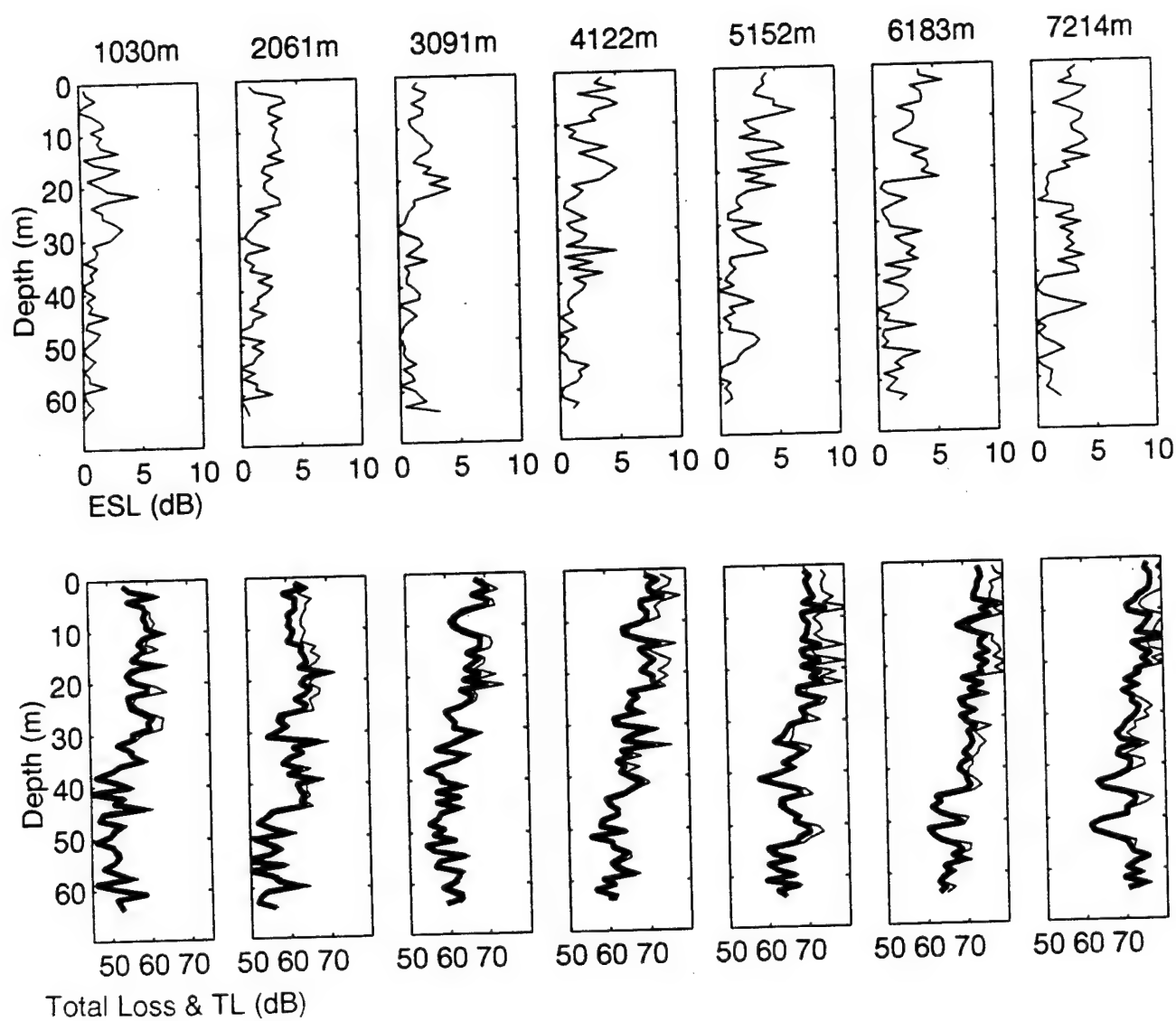
Figure 31. Same as Figure 30 except for a silt/clay bottom.
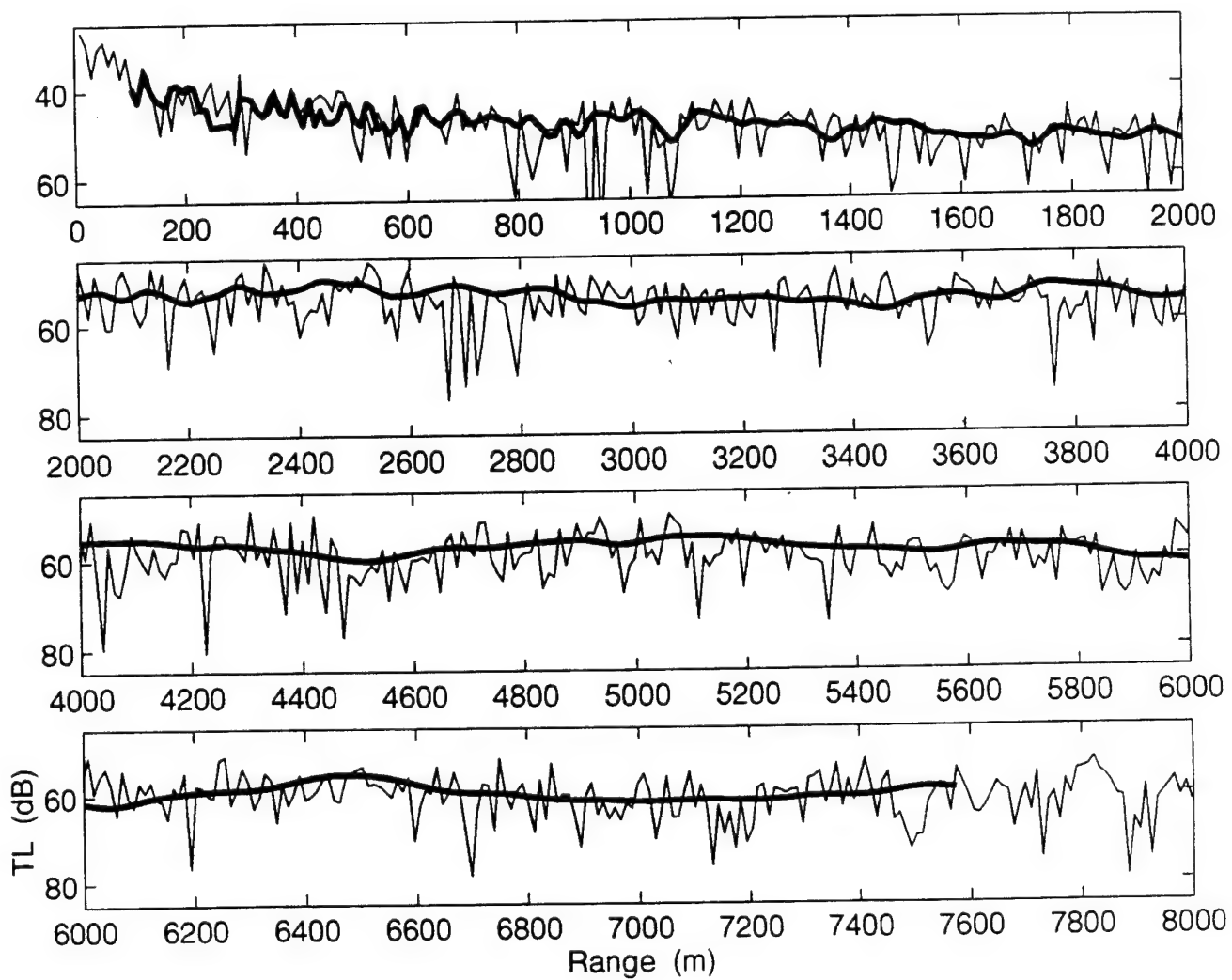
Figure 32. Comparison of TL from a single frequency (thin
line) and TL from a 200 Hz band pulse (thick line) for a
negative SSP overlying a sand bottom. Source depth is 7.3
m, target depth is 10.3 m.
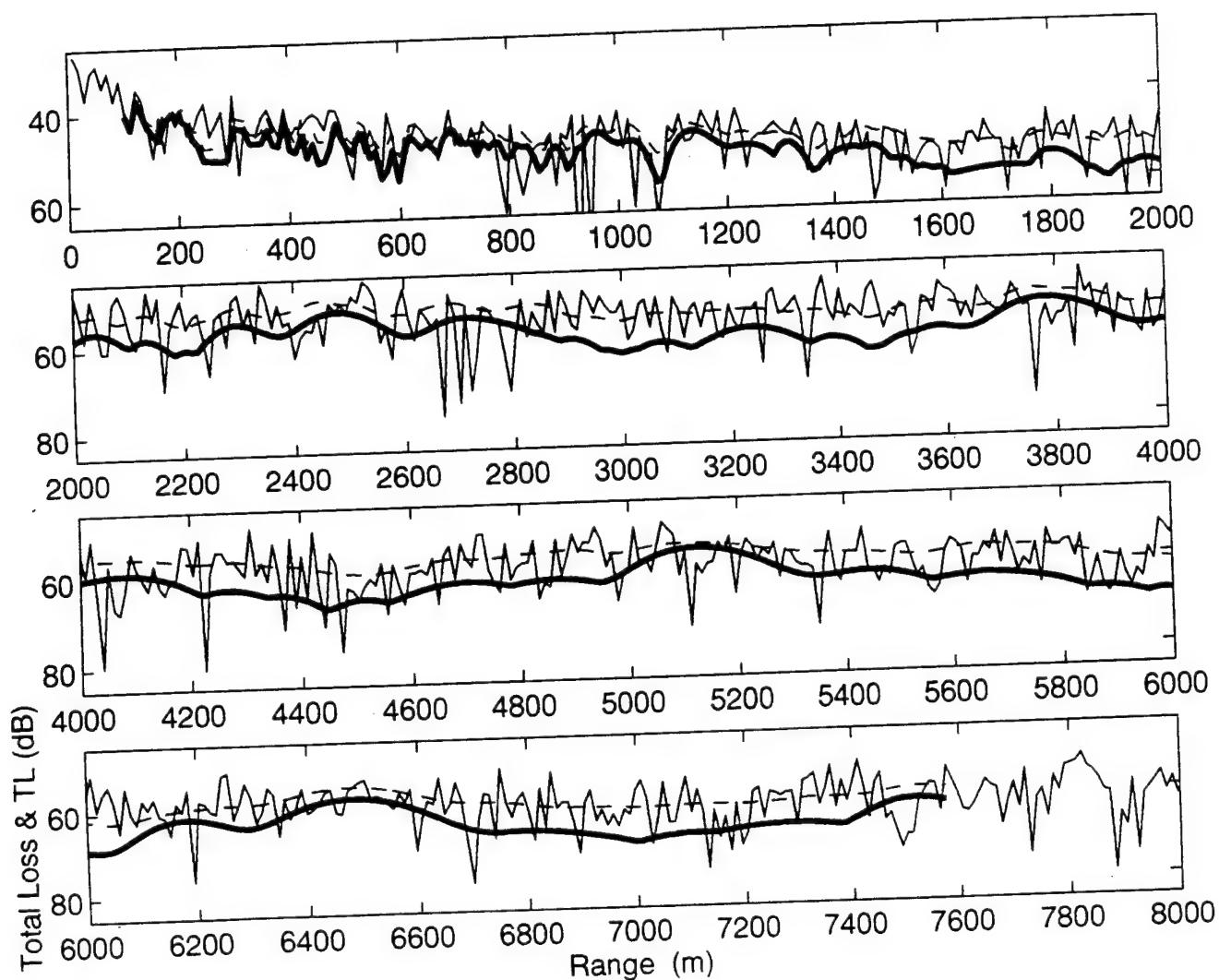
Figure 33. Comparison of TL from a single frequency (thin line) and total loss (TL + ESL) from a 200 Hz band pulse (thick line) for a negative SSP overlying a sand bottom. Source depth is 7.3 m, target depth is 10.3 m. TL from a 200 Hz band pulse (dashed line) is also shown for reference.

78

Figure 34. Comparison of ESL at 10.31 m range increment (stars) and ESL at 0.412 m range increment (solid line) for a negative SSP overlying a sand bottom. Source depth is 7.3 m, target depth is 10.3 m.

79
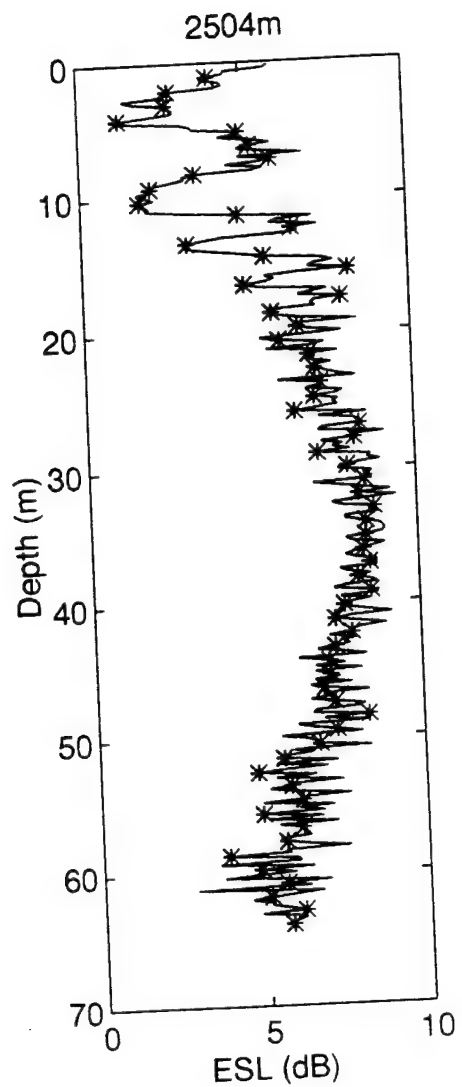
Figure 35. Comparison of ESL at 1.031 m depth increment (stars) and ESL at 0.206 m depth increment (solid line) for a negative SSP overlying sand bottom. Source depth is 7.3 m, target depth is 10.3 m.

VI. CONCLUSIONS AND RECOMMENDATIONS

A. CONCLUSION

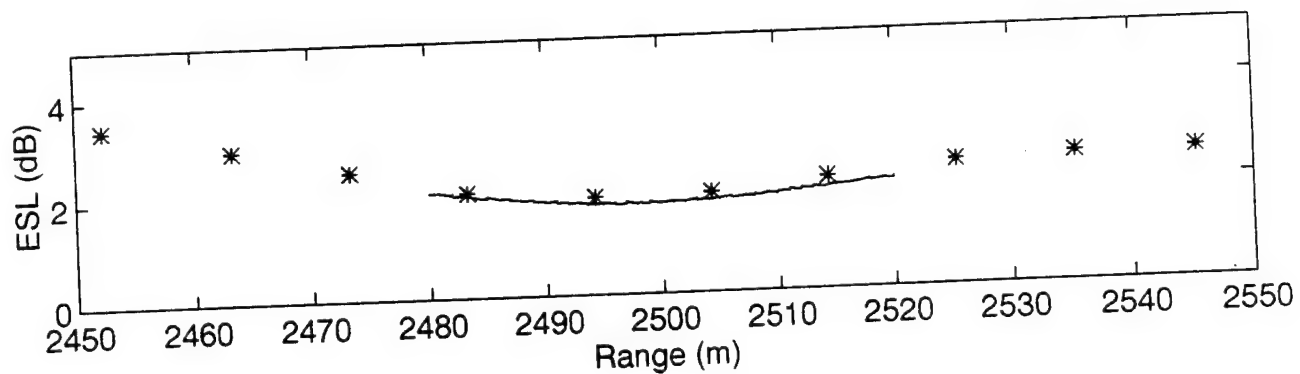- Because of the multipath nature of acoustic propagation inherent in shallow water, active sonar acoustic pulses of finite duration are stretched in time leading to a significant reduction in the peak amplitude of the returning echo. This study examined the one-way energy reduction due to time spreading, termed energy spreading loss (ESL), as a function of range, depth, source and target depth, bottom sediment composition and sound speed profile (SSP) shape. In contrast to deep water active sonar propagation, ESL in shallow water was found to be large (in excess of 10 dB for certain SSP and bottom sediment configurations) and exert a significant degradation on active sonar performance.

- The time-stretch transmitted pulse propagates in a shallow water wave guide as discrete packets or modes. The shape of the time-stretched pulse is far from the Gaussian time distribution assumed in most previous analyses.

- ESL is not a linear function of range, but increases rapidly out to a critical range (~ 1600 m

81

for the 64 m shallow area in this study) that is site dependent. Beyond this critical range ESL remains relatively constant in the mean but undergoes large-scale fluctuations (standard deviation of 1 ~ 2 dB) due to modal interference patterns. ESL is low for those range/depth combinations where most of the energy is carried by a few dominant modes propagating with nearly similar group speeds.

- ESL was determined to be predominantly dependent on the bottom sediment composition. ESL was large for propagation over highly reflective (sandy) bottoms (8 ~ 9 dB) but moderate over absorptive (silt/clay) bottoms (4 ~ 5 dB). The difference of 4 ~ 5 dB in ESL is related to the amounts of energy reflected from the bottom interface back into the water column. Highly reflective bottoms permit the propagation of both low and high order modes and their resultant variation in group speed leads to significant amounts of time stretching. Slow speed (i.e., silt/clay) absorptive bottoms attenuate the higher order modes (large angle rays which interact with the ocean boundaries), leaving only a few low order modes to propagate in the water column. The near similar group speed of these modes results in

minimal to moderate time stretching.

- In shallow water the magnitude of ESL is only weakly dependent on the SSP shape, being 1 ~ 2 dB larger for profiles exhibiting a negative, downward refracting, gradient. This weak dependency on profile shape is a characteristic feature of shallow water propagation because acoustic interaction with the upper and lower boundaries of the relatively narrow wave guide will occur regardless of the profile shape. An implication of this feature is that, for any given region, ESL is relatively invariant with season, an important tactical consideration, especially for strategic locations where current or historical SSP information may be limited or lacking.

- The transmission loss, when modeled for a single frequency (e.g., 3500 Hz in this study), exhibits rapid fluctuations of 10 ~ 20 dB along the entire propagation path due to phase interference of the propagating modes. However, when a pulse of finite bandwidth (200 Hz at 1 Hz increments centered on 3.5 kHz for this study) is modeled, the interference pattern associated with each frequency tends to average or smooth the summed TL leading to a TL curve with virtually no spatial fluctuations.

83

Overall, a higher detection probability can be anticipated from a broadband source compared to single frequency source.

- Modeling ESL accurately in shallow water allows one to quantitatively define both ESL and TL uniquely in order to assess the impact of the environment on ESL.

- ESL plus TL or total loss must be considered in assessing the impact of the environment on tactical active sonar performance. For example,

  - ESL is low and TL is high for shallow water areas with silt/clay sedimentary layers.

  - ESL is high and TL is low for shallow water areas with hard sand bottoms.

  - considering total loss (ESL + TL), tactical sonar performance is expected to be best over sand bottoms.

B. RECOMMENDATIONS

- Perform a similar analysis of the impact of the shallow water environment on ESL for transmitted pulses from advanced tactical active sonars (AN/SQS-53C and AN/SQS-22 (Active Low Frequency Sonar (ALFS))).

- Develope advanced signal processing methods, such as Inverse Beam Forming (IBF), to reduce the degradation incurred by ESL.

84

LIST OF REFERENCES

Bell, T.G. (1990). "Predicting and dealing with energy spreading loss" in Proceedings of a seminar on active sonar signal processing, 12 Dec 1989, Naval Undersea System Center, New London. Tracor Doc. T90-01-9532-U.

Chan, F. (1992). "Final report on the time spreading and energy spreading losses for the AN/SQS-53C shallow water (9/91) sea test", NUWC, New London, CT.

Collins, M.D. (1988). "FEPE user's guide", NORDA Technical Note TN-365, Naval Ocean Research and Development Activity, Stennis Space Center, MS.

Etter, P.C. (1991). "Underwater modeling: Principles, techniques, and applications", Elsevier Applied Science, New York, NY, pp 150.

Fabre, J. and Wilson, J.H. (1995). "Minimal detectable level (MDL) evaluation of inverse beam forming (IBF) using Outpost Sunrise data", submitted to J. Acoust. Soc. Am.

Hamilton, E.L. (1972). "Compressional wave attenuation in marine sediments", Geophysics, 37, 620-646.

Hamilton, E.L. (1979). "Sound velocity gradients in marine sediments", J. Acoust. Soc. Am.,65, 909-922.

Hamilton, E.L. (1980). "Geoacoustic modeling of the seafloor", J. Acoust. Soc. Am.,68, 1313-1340.

Hamilton , E.L. and Bachman, R.T. (1982). "Sound velocities and related properties of marine sediments", J. Acoust. Soc. Am.,72, 1891-1904.

Hamilton, E.L. (1985). "Sound velocity as a function of depth in marine sediments", J. Acoust. Soc. Am.,78, 1348-1355.

Hamilton, E.L. (1987). "Acoustic properties of sediments", in Acoustics and the Ocean Bottom, edited by A. Lara-Saenz, C. Ranz-Guerra and C. Carbo-Fite (Socidad Espanola de Acoustci Instituto de Acoustica - CSIC, 11 F.A.S.E. specialized conference, Madrid, Spain), pp 1-17.

Jackson, D. and Briggs, K. (1992). "High frequency bottom backscattering: roughness versus sediment volumn scattering", J. Acoust. Soc. Am., 92, 962-977.

Jensen, E.P. and Sabbadini, F. (1993). "Low frequency active sonar (LFA) bottom loss requirements", in SACLANTCEN Conference Proceedings, 24-28 May 1993, SACLANT Undersea

Research Centre, Serial no. CP-42 volume 2 of 2.

Jones, B.W. (1990). "Measurement of time spread and energy splitting" in Proceedings of a seminar on active sonar signal processing, 12 Dec 1989, Naval Undersea System Center, New London. Tracor Doc. T90-01-9532-U.

Mourad, P.D. and Jackson, D.R. (1993). "A Model/Data comparison for low frequency bottom backscatter," J. Acoust. Soc. Am. 94, 344-358.

Nuttall, A. and Wilson, J.H. (1991). "Estimation of the acoustic field directionality by use of planar and volummetric arrays via the Fourier integral method", J. Acoust. Soc. Am., 90, 2004-2019.

Rovero, P.J. (1992). "Program EXT_TD", informal program notes, Naval Postgraduate School, Monterey, CA.

Scanlon, G.A. (1995). "Estimation of bottom scattering strength from measured and modeled AN/SQS-53C reverberation levels", Master's thesis, Naval Postgraduate School, Monterey, CA.

Stewart, J.L. and Brandon, M.K. (1967). "Random medium correlation loss", Paper presented at NATO-Marina Italian

89

Advanced Study Institute on Stochastic Problems in Underwater Sound Propagation, Lerici, 18-23 Sep 1967.

Urick, R.J. (1983). "Principles of underwater sound", 3rd ed., (McGraw Hill Inc., New York, NY.), pp 237-285.

Van Trees, H.L. (1971). "Detection estimation and modulation theory", (John Wiley & Sons, Inc., New York, NY.) pp 363.

Weston, D.E. (1965). "Correlation loss in echo ranging", J. Acoust. Soc. Am., vol.37, no.1, 119-124.

Wilson J.H. (1995). "Application of inverse beam forming (IBF)", submitted to J. Acoust. Soc. Am.

Young, J.W. (1988). "A waveform and signal-processor-dependent definition of effective target strength", U.S. Navy Journal of Underwater Acoustics, vol.38, no. 2, 249-258.

INITIAL DISTRIBUTION LIST

		No. Copies
1.	Defense Technical Information Center 8725 John J. Kingman Rd., STE 0944 Ft. Belvoir, VA 22060-6218	2
2.	Dudley Knox Library Naval Postgraduate School 411 Dyer Rd. Monterey, CA 93943-5101	2
3.	Chairman (Code OC/BF) Department of Oceanography Naval Postgraduate School Monterey, CA 93943-5100	2
4.	Commanding Officer Naval Research Laboratory Code 5100/5123 Washington, D.C. 230375-5000 Attn: Dr. T.C. Yang	4
5.	Officer in Charge Naval Reseach Laboratory Stennis Space Center, MS 39529-5000 Attn: Dr. P. Bucca Dr. S. Chin-Bing Dr. D. King Mr. J. McDermid	4
6.	Commanding Officer NCCOSC RDTE DIV 53560 Hull St. San Diego, CA 92152-5100 Attn: Capt. K.E. Evans Dr. J. Roese Dr. H. Bucker Dr. F. Ryan Dr. R. Bachman	5
7.	Dr. James H. Wilson Neptune Sciences, Inc. 3834 Vista Azul San Clemente, CA 92674	12
8.	Mr. Barry Blumenthal Code C124A Office of Naval Research 800 N. Quicy St. Arlington, VA 22217-5660	1

9. ARPA/MSTO   2
    3701 N. Fairfax Dr.
    Arlington, VA 22203-1714
    Attn: Capt. Lowell
          Dr. T. Kodij

10. Mr. Ed Chaika / Mr. Dave Small   2
    Advanced Environmental Acoustic Support Program
    Code ONR-DET
    Building 1020 - Rm. 184
    Stennis Space Center, MS 39529-5000

11. Mr. John G. Schuster   1
    Technical Director
    Submarine and SSBN Security Programs
    N87/OP-02T
    Office of the Chief of Naval Operations
    Washington, D.C. 20530

12. Mr. Ed. Jensen / Mr. Al Goodman   2
    Naval Undersea Warfare Center Det., New London
    39 Smith Street
    New London, CT. 06320-5594

13. Capt. R. Goldsby / Cdr. S. Scrobo   2
    Program Executive Office
    Surface Ship ASW Systems
    Washington, D.C. 20362-5104

14. Capt. G. Nifontoff   1
    Naval Space and Warfare Command
    PD 18
    Department of the Navy
    Washington, D.C. 20245

15. Head of Plans and Program Div.   1
    Operations and Plans Department
    Maritime Staff Office, JMSDF
    9-7-5 Akasaka Minato-Ku Tokyo, Japan

16. Head of Education Div.   8
    Personnel and Education Department
    Maritime Staff Office, JMSDF
    9-7-5 Akasaka Minato-Ku Tokyo, Japan

17. Lcdr. Akira Tanaka   1
    Plans and Program Div.
    Operations and Plans Department
    Maritime Staff Office, JMSDF
    9-7-5 Akasaka Minato-Ku Tokyo, Japan